Roles of the GXXXG Motif in Amyloid Precursor Protein for Its Dimerization and Amyloid β Production

DOCTORAL DISSERTATION

The thesis submitted in partial fulfillment of the requirements for the degree of
Doctor of Philosophy

By:
Hidekazu Higashide

Supervisor:
Dr. Yasuo Ihara

Co-supervisor:
Dr. Nobuyuki Nukina

Laboratory of Cognition and Aging
Graduate School of Brain Science
Doshisha University
Kyoto, Japan
September 2018

Contents

Abstract

The amyloid β (Aβ) protein is a major component of senile plaques, which are one of the neuropathological hallmarks of Alzheimer's disease (AD). Amyloidogenic processing of amyloid precursor protein (APP) by β-secretase and γ-secretase leads to Aβ production. APP contains tandem triple repeats of the GXXXG motif (X indicates any amino acid) in its extracellular juxtamembrane and transmembrane regions. It has been reported that the GXXXG motif is related to protein–protein interactions, but it remains controversial whether this motif in APP is involved in substrate dimerization and whether such dimerization affects the γ-secretase-dependent cleavage. Here I examined the effect of amino acid substitutions within the GXXXG motifs of APP carboxyl-terminal fragment (C99) on its dimerization and Aβ production. Surprisingly, I found that substitutions in the motifs failed to alter C99 dimerization in an *in vitro* assay using detergent-solubilized substrate and blue-native PAGE. Cell-based and solubilized γ-secretase assays demonstrated that substitutions in the motif decreased the production of long Aβ species such as Aβ42 and Aβ43 and increased short Aβ species such as Aβ34. It has been proposed that C99 is initially cleaved at Aβ48 or Aβ49 and then shortened progressively by three or four residue steps depending on the 3.6-pitch alpha helical structure of C99. While this processing favors to produce Aβ40 and Aβ42 with the native C99, substitutions in the GXXXG motif may change the α-helical structure of C99 and lead to γ-secretase-cleavage shifts toward the amino terminus, thereby

resulting in the increased short Aβ such as Aβ34. My data therefore suggest that the GXXXG motifs are involved in the progressive processing of C99 by γ-secretase but not necessary for the C99 dimerization.

General Introduction

Alzheimer's disease (AD) is one of neurodegenerative diseases and the most common forms of dementia. Since AD was reported by Dr. Alois Alzheimer more than a century ago (Stelzmann *et al.* 1995), it has increased in prevalence rapidly not only in Japan but also in other developed countries. The number of people living with dementia worldwide today is estimated to be 44 million and is predicted to almost double (75.6 million) by 2030 and more than triple (135.5 million) by 2050 (Prince *et al.* 2014). The most common early symptom is difficulty in remembering recent events (short-term memory loss). As the disease advances, symptoms can include problems with disturbances in language, psychological and psychiatric changes, and impairments in activities of daily living (e.g., shopping, housekeeping, driving, cooking, managing finances, and personal care) (Burns and Iliffe 2009). There is thus an urgent need to develop therapeutics for AD.

The amyloid β (Aβ) protein is a major component of senile plaques, which are one of the neuropathological features of AD (Masters *et al.* 1985a; see also Fig. I-1A). It has been proposed that the accumulation of Aβ results in the formation of neurofibrillary tangles (NFT) (Fig. I-1A), composed of tau protein, which leads to neuronal loss and dementia (Hardy and Higgins 1992); this is referred to as "the amyloid cascade hypothesis" (Fig. I-1B). The amyloid cascade hypothesis implies that it is important to understand the mechanism of Aβ production to prevent and cure AD.

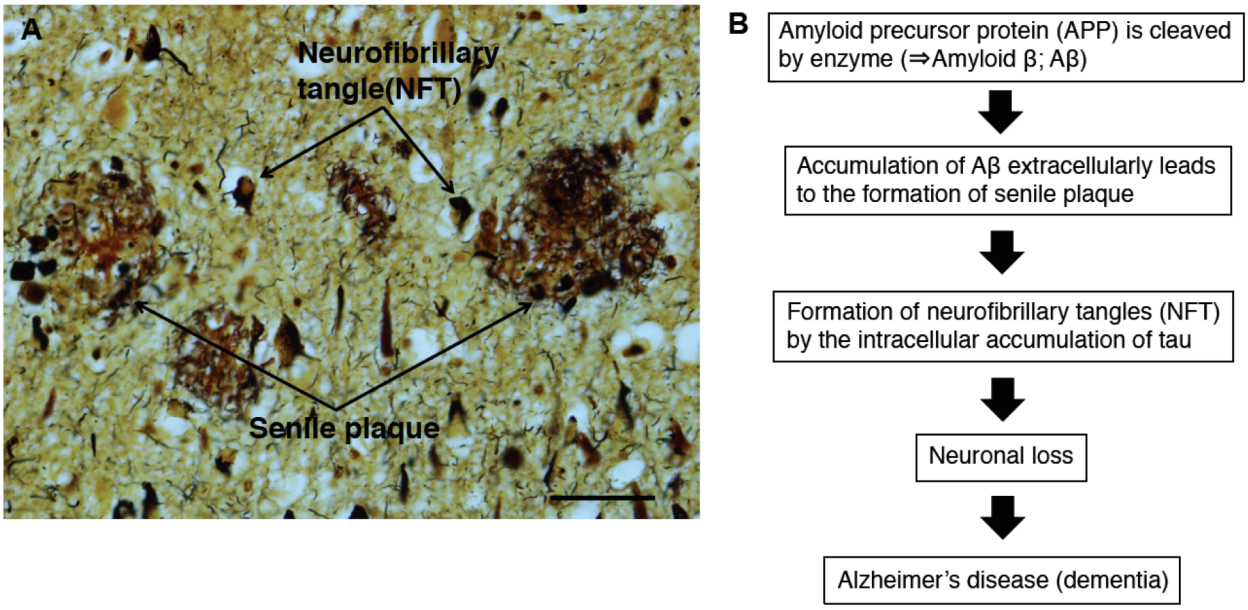

Figure I-1. Histological staining of an AD patient's brain. (A) The cortex of temporal lobe from an AD patient was stained using Bielshowsky's silver stain. The two major hallmarks of AD, senile plaques and neurofibrillary tangles (NFT) are visible. The scale bar represents 50 μm. (B) A flowchart of the amyloid cascade hypothesis. The accumulation of amyloid β (Aβ) results in the formation of senile plaques. It has been proposed that the senile plaques trigger the formation of NFT, composed of tau protein, leading to neuronal loss and dementia.

Senile plaques are one of the neuropathological features of AD. Glenner and Wong were the first to identify Aβ as the major component of senile plaques. They separated the insoluble fraction from AD brains with cerebrovascular amyloidosis by centrifugation. They extracted protein components by treating this fraction with collagenase and solubilizing them in protein denaturant guanidine-HCl and then separated them on high-performance liquid chromatography. They identified short peptides, which were later called Aβ (Glenner and Wong 1984a). Masters and colleagues also purified the cerebral amyloid protein that forms the plaque core in AD and in aged individuals with Down syndrome, and identified the same peptides reported by Glenner and Wong

(Masters *et al.* 1985a; Glenner and Wong 1984b). They predicted that these peptides are generated from a precursor protein (Masters *et al.* 1985b). This precursor protein was later identified by Kang and colleagues, who isolated and sequenced an apparently full-length complementary DNA clone coding the predicted precursor protein composed of 695 amino acids [i.e., Amyloid precursor protein (APP)] (Kang *et al.* 1987).

APP is a type-I transmembrane protein and is composed of a heterogeneous group of proteins migrating between 110 and 135 kilo dalton (kDa) on a SDS-polyacrylamide gel (Selkoe *et al.* 1988). This heterogeneity arises from alternative splicing, generating three major isoforms comprised of 695, 751, and 770 residues, as well as from a variety of posttranslational modifications (Selkoe 1994). Among the isoforms, APP751 and APP770 are widely expressed in non-neuronal cells, whereas APP695 is expressed exclusively in neurons (Haass *et al.* 1991). The primary function of APP is unknown, although it has been implicated as a regulator of synaptic formation and a factor for migration of neuronal precursors into the cortical plate during the development of the mammalian brain (Priller *et al.* 2006; Young-Pearse *et al.* 2007).

β-Secretase cleaves APP to produce the carboxyl terminal fragment of APP (C99) (Vassar *et al.* 1999; Sinha *et al.* 1999; Yan *et al.* 1999). This cleavage is referred to as β-cleavage. C99 is subsequently cleaved by γ-secretase, which results in the production of Aβ and APP intracellular domain (AICD) (Selkoe and Kopan 2003; Steiner *et al.* 2008; Thinakaran and Koo 2008; see also Fig. I-2). There are multiple species of Aβ by γ-secretase due to the promiscuity of the enzymatic cleavage. The produced Aβ ranges from 34 to 49 amino acid residues in length, while Aβ40 and Aβ42 being the major forms. Although Aβ is constitutively produced in cells (Haass *et al.* 1992; Shoji *et al.* 1992), its physiological function remains unclear. However, Aβ has been implicated as a factor of neurite-promoting matrix, as an enhancer of long-term potentiation (LTP) in rat hippocampus, and a factor of protection against microbial infection in mouse and worm models of AD (Koo *et al* 1993; Wu *et al.* 1995; Kumar *et al.* 2016).

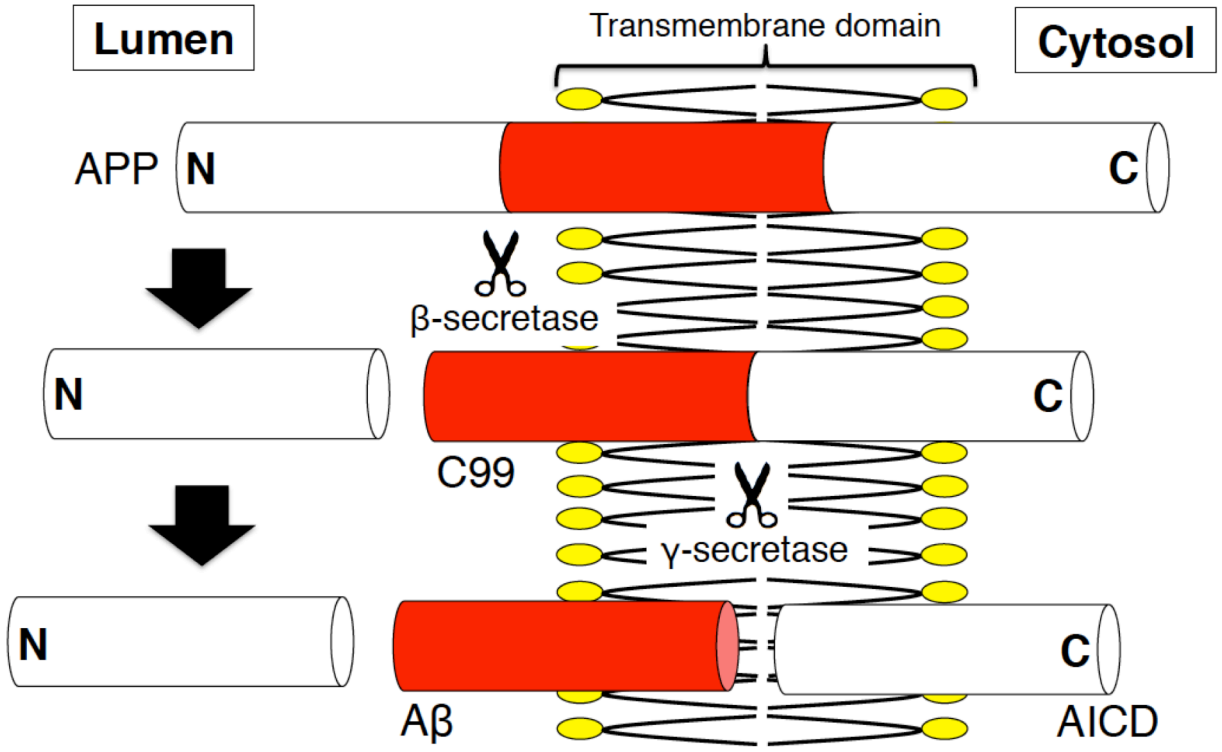

Figure I-2. Schematic representation of Aβ production. APP is cleaved by β-secretase, and thus the carboxyl terminal fragment of APP (C99) is produced. Next, C99 is cleaved by γ-secretase, which leads to the production of Aβ (red) and APP intracellular domain (AICD). Bold N and C indicate the amino terminus and carboxyl terminus, respectively.

γ-Secretase is a multi-subunit aspartic protease, composed of multiple integral membrane proteins, and cleaves single-pass transmembrane (type-I) proteins at residues within the transmembrane domain. γ-Secretase is composed of the following four membrane proteins: anterior pharynx defective-1 (Aph-1), nicastrin (Nct), presenilin enhancer-2 (Pen-2), and presenilin 1 (PS1), the last of which represents the catalytic subunit (Selkoe and Kopan 2003; Spasic and Annaert 2008; Kaether *et al.* 2006; Steiner *et al.* 2008; Lu *et al.* 2014; Francis *et al.* 2002) (Fig. I-3). APP is a substrate of γ-secretase among many others including Notch, E-cadherin, and amyloid-like

precursor proteins (APLPs) (De Strooper *et al.* 1999; Marambaud *et al.* 2002; Scheinfeld *et al.* 2002). γ-Secretase complex is thought to assemble and become active in early endoplasmic reticulum (ER) (Capell *et al.* 2005). Aph-1 and nicastrin may interact to form an immature complex prior to the assembly of the γ-secretase complex (LaVoie *et al.* 2003; Hu and Fortini 2003; Steiner *et al.* 2008). Aph-1 might be involved in stabilizing the γ-secretase complex (Takasugi *et al.* 2003; Kim *et al.* 2003; Gu *et al.* 2003; Luo *et al.* 2003; Kaether *et al.* 2006; Spasic and Annaert 2008). Pen-2 plays a role in the maturation of γ-secretase complex by promoting presenilin endoproteolysis. The mature complex is then transported into late ER compartments, where it interacts with and cleaves its substrate proteins described above (Kim *et al.* 2004).

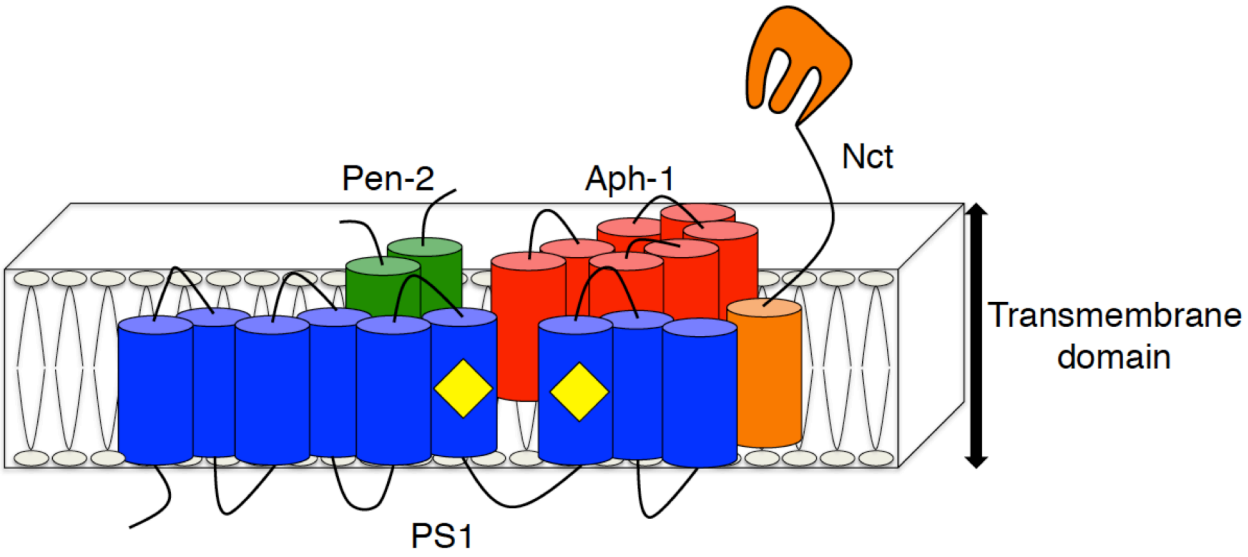

Figure I-3. Schematic representation of the γ-secretase complex. γ-Secretase acts in the intramembrane proteolysis of the C99. The minimal γ-secretase complex comprises presenilin-1 (PS1) (blue), nicastrin (Nct) (orange), anterior pharynx defective-1 (Aph-1) (red) and presenilin enhancer-2 (Pen-2) (green). Yellow rhombuses show the locations of the conserved catalytic aspartates. Aph-1 is a protein composed of 308 amino acids and acts as a regulator of the cell-surface localization of Nct (Goutte *et al.* 2002; Francis *et al.* 2002). Pen-2 is a 101-amino acid integral membrane protein (Francis *et al.* 2002). PS has a nine-transmembrane-domain topology, with the extracellular carboxyl terminus and the cytosolic amino terminus (Laudon *et al.* 2005; Spasic *et al.* 2008). Nct is a single-transmembrane glycoprotein composed of 709 amino acids, and it has been reported that Nct interacts with PS1 (Yu *et al.* 2000; Haffner *et al.* 2004; Baurac *et al.* 2003; Gu *et al.* 2003; Lee *et al.* 2002). This figure is modified from the paper by Tomita (2014).

There are many studies concerning the mechanism of γ-secretase-dependent cleavage of C99. In brief, the extracellular domain of Nct captures the most amino-terminal part of C99 as a primary substrate receptor of γ-secretase (Shah *et al.* 2005). Recently, it has been reported that γ-secretase distinguishes substrate ectodomain length and preferentially captures and cleaves substrates with a short ectodomain (Funamoto *et al.* 2013). Being captured by Nct, C99 then binds to the hydrophilic

loop 1 and the carboxyl terminus of the catalytic subunit PS1 and is incorporated into the catalytic pore (Takagi-Niidome *et al.* 2015). C99 is cleaved at sites close to the membrane/cytoplasmic boundary, which is defined as ε-cleavage, to liberate the intracellular domain (i.e., AICD) (Fig. I-4).

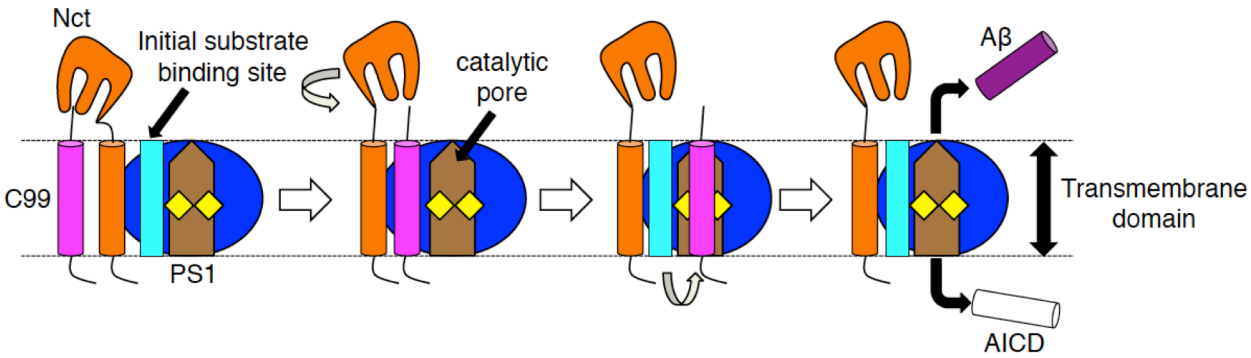

Figure I-4. Schematic model of γ-secretase-mediated intramembrane cleavage. The amino terminus of C99 (pink) is captured by the extracellular domain of Nct (orange), which guides C99 to the initial substrate-binding site (cyan box) within PS1 (blue). C99 is then transferred laterally to the catalytic pore (brown) and cleaved to release Aβ (purple) and the AICD (clear). Yellow rhombuses show the locations of the conserved catalytic aspartates. This figure is modified from the paper by Tomita (2014).

This ε-cleavage results in the production of Aβ48 or Aβ49 (Gu *et al.*, 2001), which are then processed successively by γ-secretase, three to four residues at a time (i.e., ζ-cleavage and γ-cleavage) (Qi-Takahara *et al.* 2005; Zhao *et al.* 2004) to produce multiple species of Aβ. Qi-Takahara and colleagues identified longer Aβ species than the major Aβ40 and Aβ42 forms, such as Aβ48, Aβ46, Aβ45, and Aβ43 in the cell lysate (Qi-Takahara *et al.* 2005). They also found that treatment of cells with a γ-secretase inhibitor resulted in the intracellular accumulation of

longer Aβ species together with the reduction of Aβ40 and Aβ42 in the culture medium. Reduction of intracellular Aβ40 is associated with the accumulation of intracellular Aβ43 at a low dosage of the inhibitor and of intracellular Aβ46 at a higher dosage (Qi-Takahara *et al.* 2005). These findings suggest that Aβ43 is produced from Aβ46, and that Aβ43 is the precursor of Aβ40.

The transmembrane domain of C99 is postulated to adopt an α-helix that needs 3.6 residues for one complete turn (Lichtenthaler *et al.* 1999b). Based on this model, Qi-Takahara and colleagues proposed that the cleavage sites for Aβ49, Aβ46, Aβ43, and Aβ40 are aligned on the α-helical surface of the C99 molecule, whereas those for Aβ48, Aβ45, and Aβ42 are aligned on another α-helical surface (Fig. I-5) (Qi-Takahara *et al.* 2005). They therefore hypothesized that γ-secretase removes three or four residues sequentially from the initial products Aβ48 or Aβ49 to produce shorter Aβ species. Takami and colleagues did confirm that Aβ49 is converted to Aβ43 and Aβ40 by the sequential release of two or three tripeptides (i.e., Aβ49 > Aβ46 > Aβ43 > Aβ40) and that Aβ48 is converted to Aβ42 and Aβ38 by the sequential release of two tripeptides or these plus an additional tetrapeptide (i.e., Aβ48 > Aβ45 > Aβ42 > Aβ38) (Fig. I-6) (Takami *et al.* 2009).

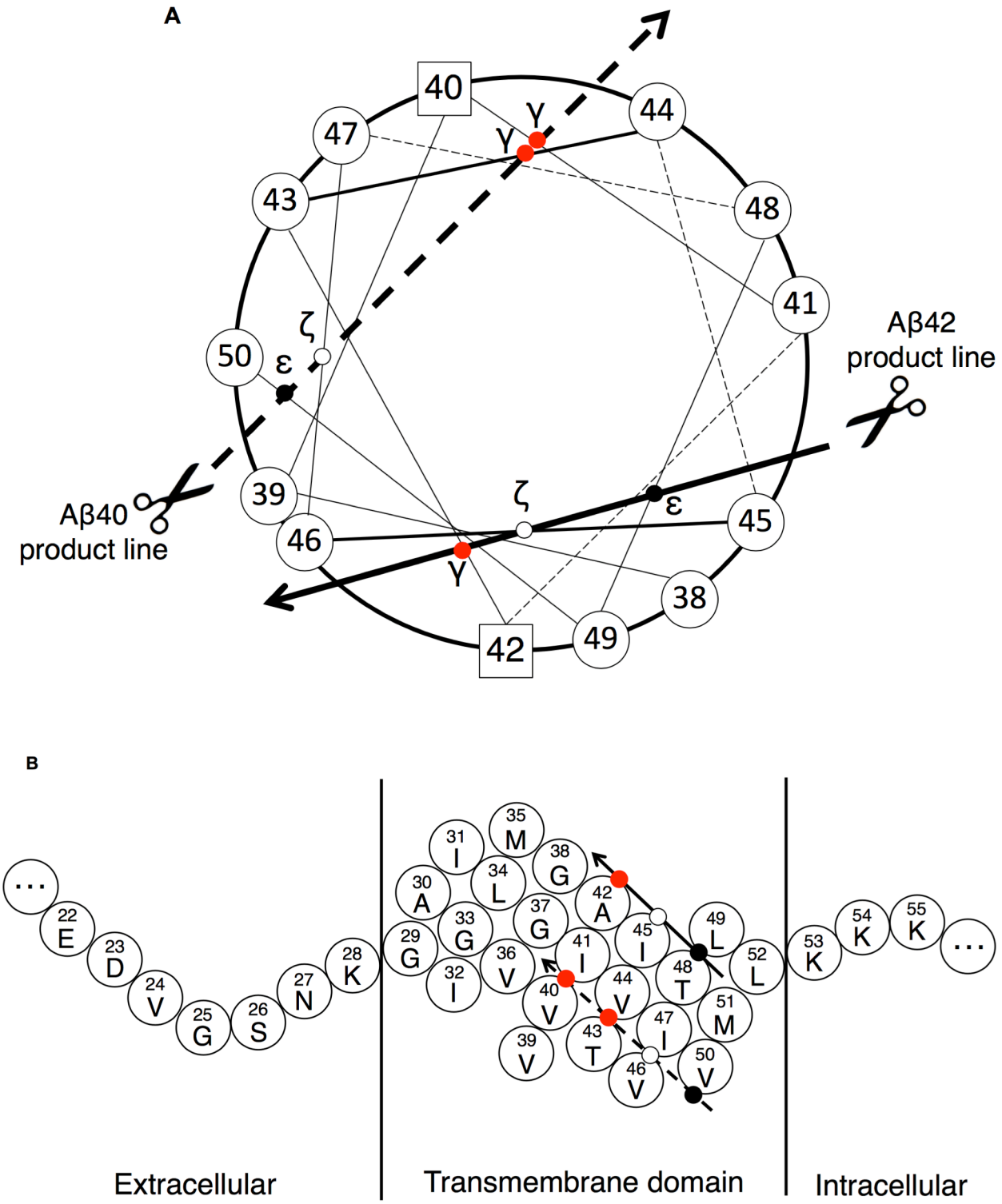
A
40
44
47
43
48
41
50
39
46
45
38
49
42
γ
γ
ζ
ε
ζ
ε
γ
Aβ42
product line
Aβ40
product line
B
...
22
E
23
D
24
V
25
G
26
S
27
N
28
K
29
G
30
A
31
I
32
I
33
G
34
L
35
M
36
V
37
G
38
G
39
V
40
V
41
I
42
A
43
T
44
V
45
I
46
V
47
I
48
T
49
L
50
V
51
M
52
L
53
K
54
K
55
K
...
Extracellular
Transmembrane domain
Intracellular

Figure I-5. Schematic representation of an α-helical model of C99 and γ-secretase cleavage sites. (A) A view from the luminal side on the α-helix wheel representing a carboxyl half of the transmembrane domain of APP. The numbers indicate the amino acid sequence of Aβ. The cleavage sites for the generation of Aβ40 and Aβ42 (indicated by the dotted and solid arrows, respectively) are topographically in the opposite directions relative to the α-helical surface of the transmembrane domain. The carboxyl sides of V-46 and T-43 are aligned with that of V-40 on the same side of the α-helical surface, whereas those of T-48 and I-45 are aligned with that of A-42 on the opposite side. Solid and dotted lines represent cleaved peptide bonds by γ-secretase and intact bonds, respectively. (B) A side view on the α-helix of the transmembrane domain of APP. The number at the top and the letter at the bottom represent Aβ numbering and amino acid, respectively. The cleavage sites for generation of Aβ40 and Aβ42 are distinctly aligned (indicated by dotted arrow and arrow, respectively) on the surface of the α-helix of the transmembrane domain. Black circle, white circle, and red circle represent ε-cleavage, ζ-cleavage, and γ-cleavage, respectively. These figures are modified from the paper by Qi-Takahara *et al.* (2005).

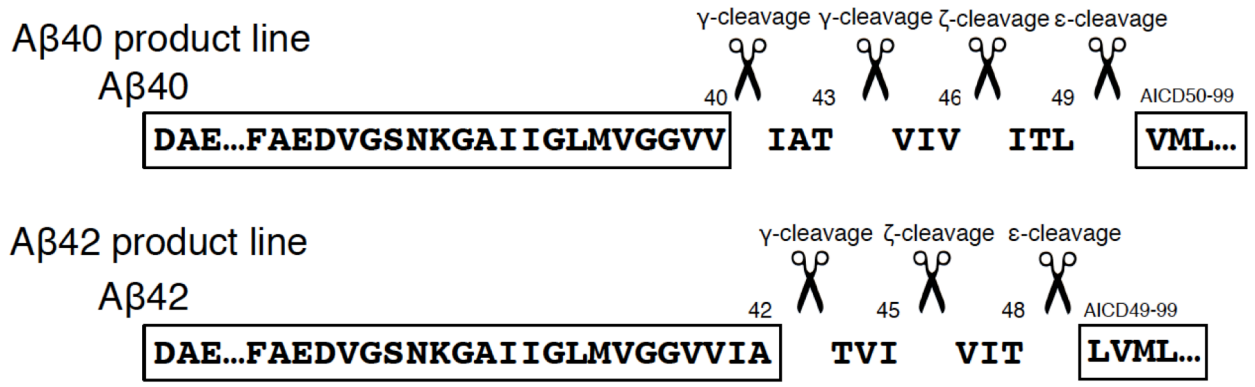

Figure I-6. Schematic representation of γ-secretase-mediated successive tripeptide release from C99. ε-Cleavage at the membrane–cytoplasmic boundary of C99 generates Aβ49 and Aβ48 and their counterparts AICD50-99 and AICD49-99 (boxed), respectively. The number represents Aβ numbering. γ-Secretase then successively cleaves in a direction from the ε-cleavage (right scissors) to γ-cleavage sites (left scissors) Aβ49 and Aβ48 by releasing tripeptides at every helical turn, finally producing Aβ40 and Aβ42, respectively. Thus, the processing of Aβ49 accompanies the release of ITL, VIV, and IAT in this order, whereas that of Aβ48 accompanies the release of VIT, followed by TVI. This figure is modified from the paper by Takami *et al.* (2009).

Among the secreted Aβ species, Aβ40 is the major Aβ species produced by cells (~90%), whereas Aβ42 is a minor species (~10%). Despite being minor, Aβ42 is the major component of senile plaques that are thought to be amyloidogenic and possess cell toxicity (Iwatsubo *et al.* 1994; Younkin 1995). Therefore, it is proposed that it is critical to decrease the level of Aβ42 to treat and prevent AD. However, the mechanism of Aβ42 production remains unclear. Thus, it is important to elucidate how APP is processed by γ-secretase. Modulation of this processing may help to develop therapeutic strategies to inhibit the production of Aβ42 specifically without inhibiting the processing of other substrates of γ-secretase, which may cause serious adverse effects.

In this thesis research, I therefore studied the structural determinants, which would affect how amyloidogenic Aβ42 production is regulated. Recent studies proposed that GXXXG motifs (X represents any amino acid) present in APP/C99 induce their homo-dimerization and modulate the Aβ42 production by γ-secretase. Since the effects of GXXXG motif on dimerization and Aβ production remain controversial to date, I investigated whether these GXXXG motifs really facilitate the dimerization and if that affects the production of Aβ.

Chapter Ⅰ.

Effect of amino acid substitutions in the GXXXG motifs of C99 on its dimerization *in vitro*

Introduction

Furthmayr and Marchesi discovered that human glycophorin A (GpA) transmembrane domain is responsible for its dimerization (Furthmayr and Marchesi 1976). GpA has a GXXXG motif and it has been implicated in transmembrane domain interactions for many proteins [e.g., E-cadherin and Amyloid-like protein-1 (APLP-1)] (Russ and Engelman 2000; Troyanovsky *et al.* 2003; Soba *et al.* 2006). Aph-1, one of the γ-secretase components, also has two consecutive GXXXG motifs within the transmembrane domain 4. It has been reported that the interaction via the GXXXG motifs of Aph-1 with presenilins is critical for the protein stability and the activity of the γ-secretase complex (Araki *et al.* 2006; Niimura *et al.* 2005; Lee *et al.* 2004).

APP also contains three GXXXG motifs in the extracellular juxtamembrane and transmembrane regions (Fig. 1-1). It has been reported that these motifs are involved in the dimerization of APP and C99 (Munter *et al.* 2007; Kienlen-Campard *et al.* 2008). However, since the previous studies used an artificial substrate (Aβ29-42) or focused on SDS-resistant dimerization, it is unclear whether C99 forms dimers in the physiological condition via the GXXXG motifs. Because the substrate dimerization can potentially impact the substrate recognition by γ-secretase, stability of the binding, and the proteolytic processing, I aimed to test whether the GXXXG motifs in C99 are critical in the dimerization.

In this study, I applied the blue native polyacrylamide gel electrophoresis (BN-PAGE) technique to examine the effect of amino acid substitutions in the GXXXG motifs on C99 dimerization. BN-PAGE is an ideal approach to examine the state of protein–protein interactions because it allows the separation of protein complexes without interfering with intra-protein and extra-protein interactions (Schägger and Jagow 1991; Schägger 2001; Schägger *et al.* 1994; Wittig *et al.* 2006).

Materials and Methods

DNA Oligonucleotides

The oligonucleotides to generate C99 mutants used in this study were described in Table 1.

Antibodies

In this study, anti-human Aβ antibody 82E1 (IBL) was used to visualize and quantify C99 in Western blotting. 82E1 is specific to the amino-terminal end of human Aβ (Fig. 1-2) and therefore expected to detect C99.

Cell Culture

Sf9 cells were cultured in Gibco® Sf-900™ Ⅲ SFM 1× (Serum Free Medium Complete) (Invitrogen) at 27.5°C. Sf9 cells, a clonal isolate of *Spodoptera frugiperda* Sf21 cells (IPLB-SF21-AE), are insect cells, which are commonly available for recombinant protein production using baculovirus. It has been reported that Sf9 cells transfected with APP695 or C99 did not produce Aβ, although APP was cleaved by β-secretase to produce C99, which is tightly bound to human presenilin 1, the potential catalytic subunit of γ-secretase (Pitsi *et al.* 2002).

Preparation of C99-FLAG Substrates

FLAG-tagged C99 was prepared, in accordance with a previously reported protocol (Kakuda *et al*. 2006). In detail, a CTF of APP (C99) was carboxyl-terminally fused with the FLAG tag (DYKDDDDK) (C99-FLAG) and amino-terminally with the signal peptide of human α-galactosidase A (MQLRNPELHLGCALALRFLALVSWDIPGARA). For C99 mutants [refer to here as 3G, 2G, 1G, 0G (A), 0G (L), and 0G (F)] (see Fig. 1-1), the plasmid was amplified by PCR using the primers listed in Table 1. The mutations were confirmed by DNA sequencing, using 3130xl Genetic Analyzers (Thermo Fisher Scientific). The resultant fragments were inserted into pFastBac™ plasmid (Invitrogen). The plasmid was introduced into Sf9 cells by transfection, in accordance with the manufacturer's instructions. After transfection, recombinant baculovirus in the cell culture medium was collected. Next, Sf9 cells were infected with the recombinant baculovirus. Infected cells were harvested after 36 h. The cells were mixed with the lysis buffer [50 mM Tris-HCl, pH 7.6, 150 mM NaCl, 2% Nonidet-P 40 and 2× protease inhibitor mixture (Roche Diagnostics)] and incubated at 4°C for 30 min. After ultracentrifugation at 36,000 rpm and 4°C for 60 min, the supernatant was agitated with 5 ml of ANTI-FLAG® M2-agarose beads (Sigma−Aldrich) for WT, 3G, 2G, 1G, and 0G (A), and Anti DYKDDDDK tag Antibody Beads (WAKO) for 0G (L) and 0G (F) overnight. Bound proteins were eluted from the beads by 5 ml of Elution Buffer (0.2 M glycine HCl containing 0.3% of Nonidet-P 40, pH 2.5), and the eluate was

immediately neutralized by the addition of 1/10 volume of 3 M Tris-HCl, pH 8.0. The proteins were separated in a SDS-gel and stained with Coomassie Brilliant Blue (CBB) to test for purity (Fig. 1-3).

Blue native polyacrylamide gel electrophoresis (BN-PAGE) and two-dimensional (2D) PAGE Analyses

BN-PAGE is a native PAGE technique to analyze proteins without denaturing, and therefore widely used to analyze protein-protein interactions. The procedures for BN-PAGE were as follows: A 1/10 volume of 10% n-dodecyl-β-D-maltoside (DDM) (Invitrogen) was added to each C99-FLAG substrate solution, and then mixed with NativePAGE™ Sample Buffer (4×) (Invitrogen) and 1/5 volume of NativePAGE™ 5% G-250 Sample Additive (Invitrogen). The samples were separated on a 10% Tris−Tricine gel without sodium dodecyl sulfate (SDS). For electrophoresis, anode and cathode buffers were prepared from NativePAGE™ Running Buffer (20×) (Invitrogen). The cathode buffer (1×) contained 0.1× NativePAGE™ Cathode Buffer Additive (20×) (Invitrogen). Gels were run at a constant voltage of 150 V at 4°C.

I also performed BN-SDS 2D PAGE (see Results). For this, the BN gel strip was equilibrated with NuPAGE® LDS Sample Buffer (Invitrogen), in accordance with the manufacturer's instructions. In detail, the gel strip was incubated in a Reducing Solution [1×

NuPAGE® LDS Sample Buffer containing 1/10 volume of 10× NuPAGE® Sample Reducing Agent (Invitrogen)], then an Alkylating Solution [1× NuPAGE® LDS Sample Buffer containing 50 mM N,N-dimethylacrylamide (DMA) (Sigma-Aldrich)], and finally a Quenching Solution (1× NuPAGE® LDS Sample Buffer containing 1× NuPAGE® Sample Reducing Agent and 20% ethanol) at room temperature for 30 min each. The equilibrated gel strip was applied onto a 12% Tris−Tricine gel containing SDS, and SDS-PAGE was performed.

Proteins separated in 1D and 2D gels were electrophoretically transferred onto polyvinylidene difluoride (PVDF) membranes (0.2 μm pore size) (Pall Life Sciences). All blots were boiled in phosphate-buffered saline (PBS) (137 mM NaCl, 2.7 mM KCl, 8.1 mM Na_2HPO_4, and 1.47 mM KH_2PO_4) for 4 min to facilitate immunodetection (Swerdlow *et al.* 1986; Ida *et al.* 1996), and were then blocked in 5%−10% skim milk in Tris-buffered saline (TBS) (50 mM Tris-HCl, 150 mM NaCl, pH 7.6) containing 0.1% polyoxyethylene sorbitan monolaurate (Tween 20) for 30 min. 82E1 antibody was used to detect monomers, dimers, and trimers of C99.

Statistical Analysis

Band intensity was quantified using a LAS-4000 luminescent image analyzer (Fujifilm). Holm−Sidak's post hoc test was used to compare the relative abundance of the monomers and multimers of C99 mutants with that of C99 WT. All data are shown as mean ± standard error of the mean (SEM), and statistical significance was assessed at $p < 0.05$.

Results

To investigate whether the GXXXG motif is involved in the dimerization of the full-length substrate C99, alanine residues in the motifs were substituted at position(s) G37, G33/37, G29/33/37, and G25/29/33/37 in C99-FLAG [referred to as 3G, 2G, 1G, and 0G (A), respectively] (Fig. 1-1). These recombinants were expressed in Sf9 cells using recombinant baculovirus and purified as described previously (Kakuda *et al.* 2006; see also Materials and Methods). They were then separated on a SDS gel and stained with CBB to verify the purity and quantify the levels with BSA as standard (Fig. 1-3). Although there were protein bands other than C99-FLAG (and the putative IgG bands at 26 kDa and 50 kDa), they were not detectable with the antibody 82E1 (data not shown). The molecular weight bands at about 15 kDa and at about 11 kDa before incubation represent probably amino-terminally extended C99-FLAG with residual signal peptide and carboxyl-terminally truncated C99-FLAG, respectively (Kakuda *et al.* 2006).

To test if C99 forms dimers and whether the amino acid substitutions in the GXXXG motifs affect it, equal amounts of C99 wild type (WT) and mutants were subjected to BN-PAGE followed by immunochemical detection. As shown in Fig. 1-4A, C99 WT exhibited higher molecular weight bands than that corresponding to monomeric C99. These bands are multimers containing C99 because the addition of SDS collapsed all bands to a single band with the molecular weight of monomeric C99. This was also confirmed by BN-SDS 2D PAGE (Fig. 1-5), in which

proteins in the bands in the BN gel were separated in a SDS gel in a denatured condition. All the immunoreactive proteins appeared at apparently 15 kDa bands, which again correspond to the size of monomeric C99. While I cannot exclude the possibility that C99 forms multimers with other protein contaminants in the sample, I assumed that the immunoreactive bands at apparently 30 kDa and 45 kDa in a BN gel represents those of dimeric and trimeric C99.

Next, to test whether the amino acid substitutions in the GXXXG motifs affect this multimerization, the C99 mutants were subjected to the BN-PAGE and Western blotting. Surprisingly, no apparent differences were observed between WT and any alanine mutant in the formation of multimers (Fig. 1-4A). Quantification of the ratios of the monomer, the dimer, and the trimer also showed no significant differences (Fig. 1-4C).

One possible interpretation for this lack of significant changes in the multimeric formation of C99 is structural or size similarity between glycine and alanine residues, such that the function of GXXXG was retained even in AXXXA. To test this possibility, I performed leucine or phenylalanine substitutions at positions G25/29/33/37 in the motif of C99-FLAG [referred to as 0G (L) and 0G (F), respectively] (see Fig. 1-1). I found no effect of the leucine and phenylalanine substitutions on C99 dimerization (Fig. 1-4B and D). It should be noted that all of these mutants still bind to γ-secretase components and are good substrates for the γ-secretase cleavage (see Chapter II). Taken together, these findings indicate that the GXXXG motifs of C99 are not crucial

for the formation of C99 dimers and trimers.

Discussion

GXXXG and GXXXG-like motifs (e.g., small-XXX-small motifs, where small indicates amino acid residues with small side-chains like glycine, alanine, and serine), also called as glycine zipper motifs, have been implicated in the inter-helix binding or transmembrane helix packing. (Russ and Engelman 2000). For example, the GXXXG motifs on Aph-1 are known to be involved in the assembly of the γ-secretase complex and the maturation of the components (Lee *et al.* 2004). Mutants of the GXXXG motif and GXXXG-like motifs on γ-secretase subunits [e.g., Aph-1 within transmembrane domain 4 (GXXXGXXXG) and presenilin within transmembrane domain 8 (AXXXAXXXG)] disrupt the assembly and activity of the γ-secretase complex (Lee *et al.* 2004; Marinangeli *et al.* 2015).

Previous studies have shown that the GXXXG motifs in C99 are also critical in its homo-dimerization, although there have been controversial reports. In this study, using BN-PAGE, I demonstrated that substituting Gly to Ala, Leu, or Phe did not alter the levels of C99 dimers and trimers *in vitro* (Fig. 1-4). This is consistent with the recent reports that mutating the $G_{29}XXXG_{33}$ did not affect dimerization (Decock *et al.* 2016) and that the TVIV sequence near a γ-cleavage site is critical for homo-dimerization (Yan *et al.* 2017). Although my results do not exclude the possibility that the mutations alter the affinity of the interaction, I conclude that the GXXXG motifs are not absolutely necessary for the multimerization of C99.

Figures

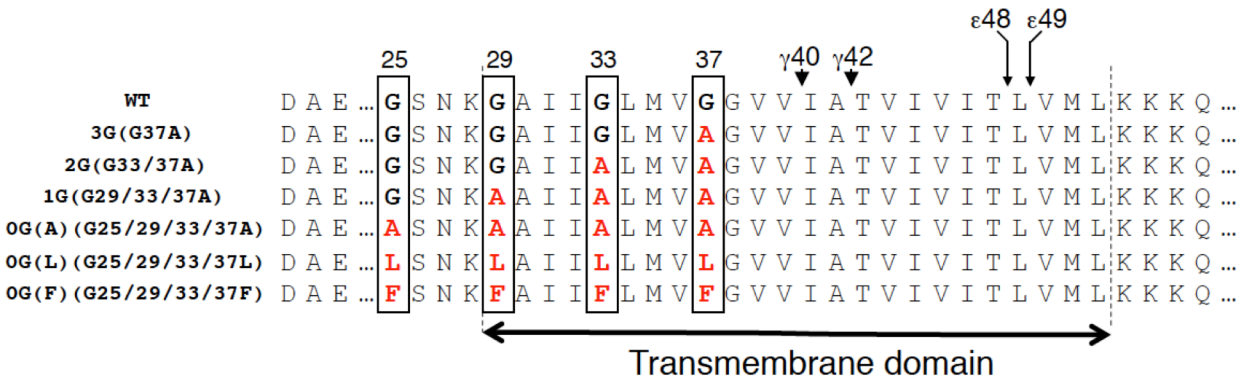

Figure 1-1. Schematic representation of substitutions in C99-FLAG substrate. C99 contains three tandem GXXXG motifs in its extracellular juxtamembrane and transmembrane regions. The number represents Aβ numbering. Rectangles, arrowheads and arrows represent the G of the GXXXG motifs, γ-cleavage site and ε-cleavage site, respectively. A, L, and F in red indicate each substitution in the GXXXG motifs.

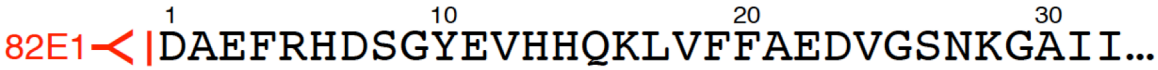

Figure 1-2. Immunoactivity of anti-Aβ antibody. Recognition site of anti-Aβ antibody in the human C99/Aβ sequence. The number represents Aβ numbering. 82E1 is specific to the amino-terminal end of human Aβ. Therefore, it is very useful to detect APP fragments generated by β-secretase cleavage.

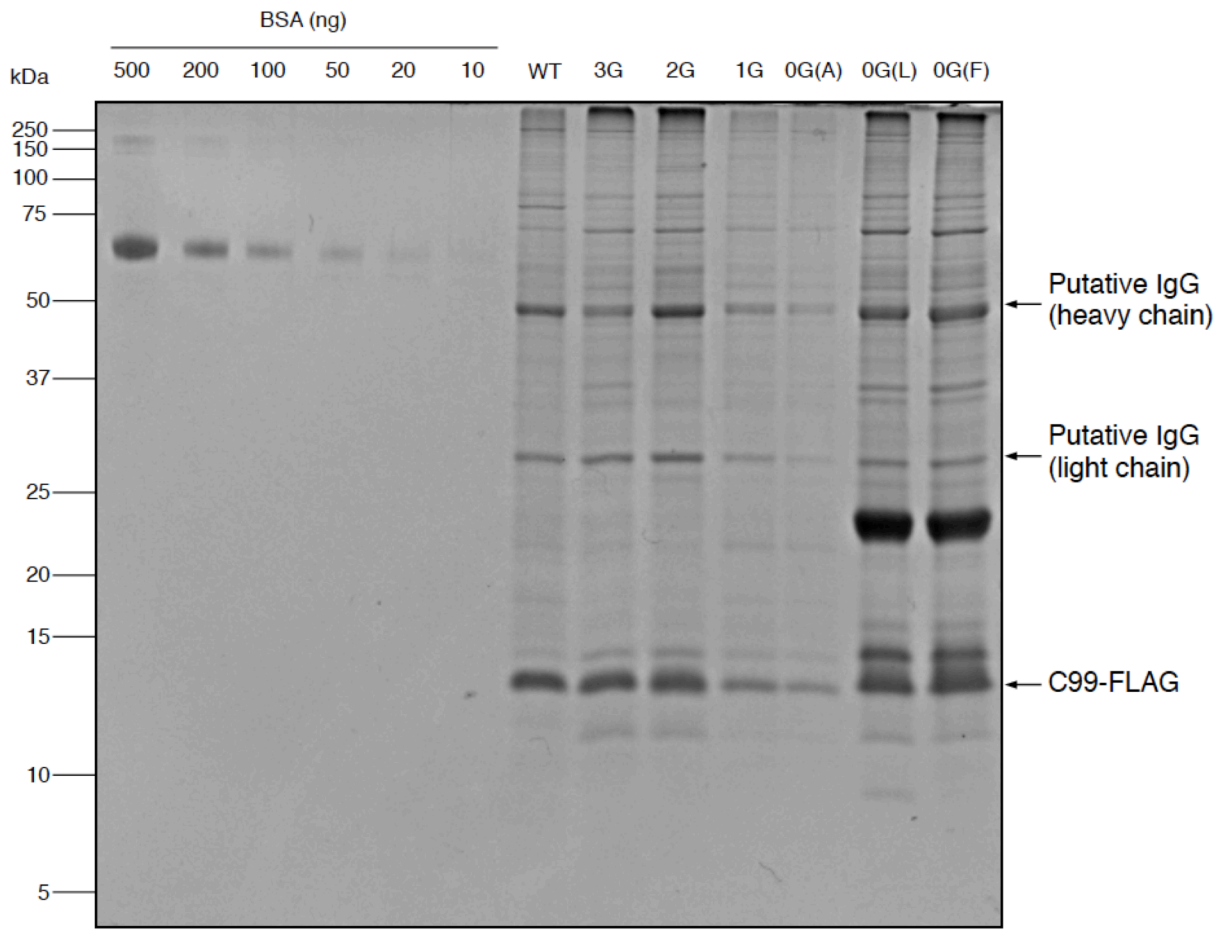

Figure 1-3. Analysis of protein purity by Coomassie Brilliant Blue (CBB) staining. Elute of C99 was subjected to CBB staining after gel electrophoresis. Although there were protein bands other than C99-FLAG (and the putative IgG light chain band at 26 kDa and the putative IgG heavy chain band at 50 kDa), they were not detectable with the antibody 82E1 (data not shown). The band intensities of bovine serum albumin (BSA) as a standard and C99-FLAG were measured using LAS-4000 luminescent image analyzer. Each C99-FLAG concentration was quantified according to a calibration curve using the intensity of BSA.

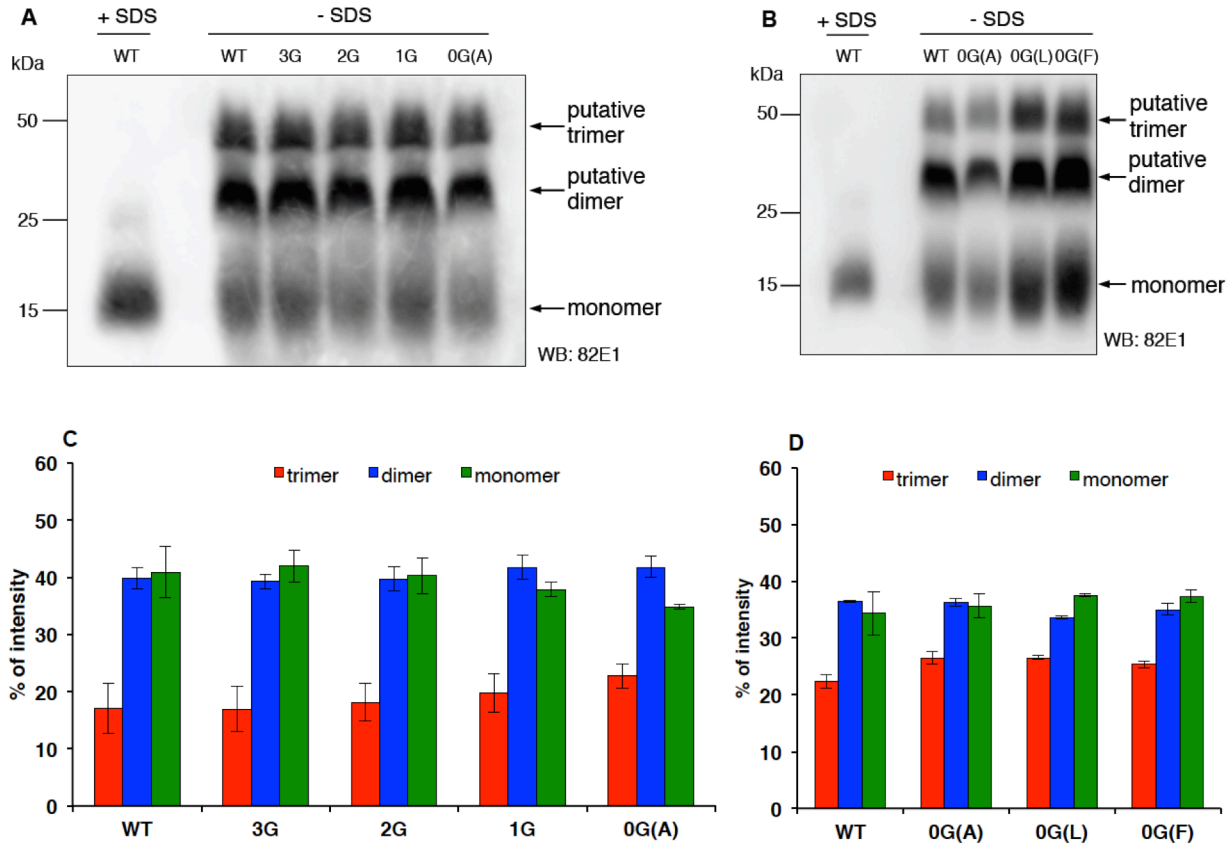

Figure 1-4. Analysis of substrate dimerization by blue native polyacrylamide gel electrophoresis (BN-PAGE). (A and B) C99-FLAG substrates were separated by BN-PAGE. Monomer, dimer, and trimer of the C99-FLAG substrates were visualized using 82E1 antibody. In the presence of sodium dodecyl sulfate (SDS ; +SDS), C99-FLAG appeared at approximately 15 kDa, as seen in SDS-PAGE, indicating the monomeric C99-FLAG band. (C and D) The intensity of each monomeric, dimeric, and trimeric band was measured using a LAS 4000 luminescent image analyzer. The percentage of each band was calculated as the sum of all with the peak intensity set at 100%. No significant differences were detected between these bands. Data are expressed as mean ± SEM (n = 3, ANOVA with Holm−Sidak's post hoc test compared with wild type; WT).

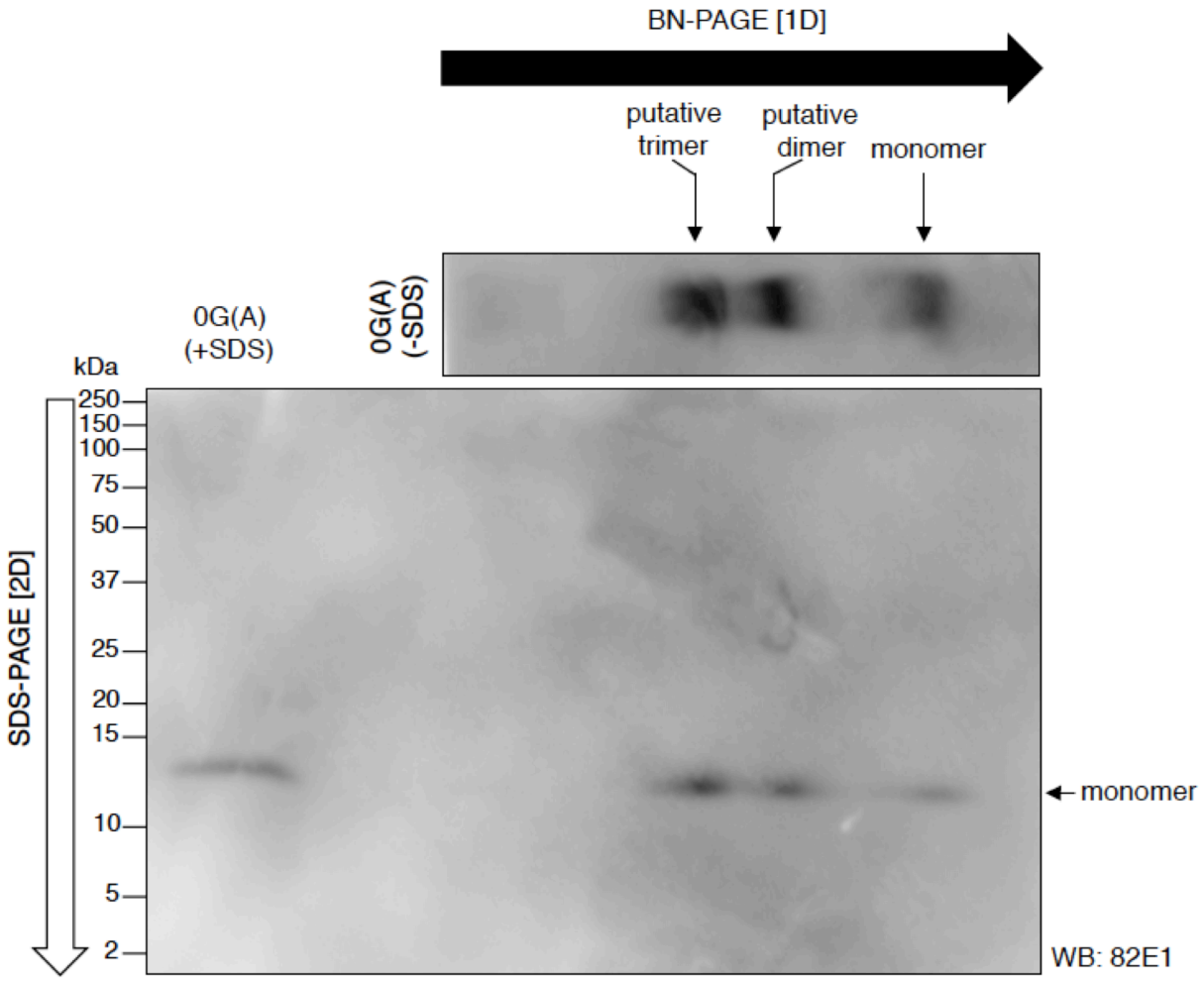

Figure 1-5. Two-dimensional gel analysis of C99-FLAG substrate. 0G (A) substrate was separated on BN-PAGE (1D). The gel was run at a constant voltage of 150 V at 4°C. The blue native gel strip was equilibrated, in accordance with the manufacturer's instructions and applied to SDS-PAGE (2D). SDS-PAGE was performed as described in Materials and Methods. Dimer and trimer bands detected in BN-PAGE were dissociated into monomer in SDS-PAGE. 0G (A) substrate in the presence of SDS (+SDS) was loaded as a positive control. Bands were detected by 82E1 antibody.

Table

primer name	Oligonucleotides
G25A-forward	5′-CAGAAGATGTGGCTTCAAACAAAGC-3′
G25A-reverse	5′-GCTTTGTTTGAAGCCACATCTTCTG-3′
G29A-forward	5′-GTTCAAACAAAGCTGCAATCATTGG-3′
G29A-reverse	5′-CCAATGATTGCAGCTTTGTTTGAAC-3′
G33A-forward	5′-GTGCAATCATTGCACTCATGGTGGG-3′
G33A-reverse	5′-CCCACCATGAGTGCAATGATTGCAC-3′
G37A-forward	5′-CACTCATGGTGGCCGGTGTTGTCAT-3′
G37A-reverse	5′-ATGACAACACCGGCCACCATGAGTG-3′
0G(L)-forward	5′-GCAGAAGATGTGCTTTCAAACAAACTTGCAA-TCATTCTACTCATGGTGCTCGGTGTTGTCATA-3′
0G(L)-reverse	5′-TATGACAACACCGAGCACCATGAGTAGAATG-ATTGCAAGTTTGTTTGAAAGCACATCTTCTGC-3′
0G(F)-forward	5′-GCAGAAGATGTGTTTTCAAACAAATTTGCAA-TCATTTTCCTCATGGTGTTCGGTGTTGTCATA-3′
0G(F)-reverse	5′-TATGACAACACCGAACACCATGAGGAAAATG-ATTGCAAATTTGTTTGAAAACACATCTTCTGC-3′

Table 1. List of oligonucleotides used in this study.

Chapter Ⅱ.

Amino acid substitutions in the GXXXG motifs alter the successive triplet cleavage of C99 by γ-secretase

Introduction

Previous studies reported that the GXXXG motifs are involved in the dimerization of C99 and affects its processing by γ-secretase. However, the effects of mutations in the GXXXG motifs on dimerization and Aβ production are controversial. Munter and colleagues reported that alanine substitutions in the GXXXG motifs of Aβ29-42 attenuate its dimerization. The same substitutions in the full-length APP results in a decrease in the production of Aβ42, while increasing the production of short Aβ species (i.e., Aβ34, Aβ35, Aβ37, and Aβ38) in a cellular assay (Munter *et al.* 2007). In contrast, Kienlen-Campard and colleagues reported that leucine substitutions in the GXXXG motifs promote C99 dimerization and decrease the levels of both Aβ40 and Aβ42 in cells (Kienlen-Campard *et al.* 2008). Nevertheless, the consensus is that the GXXXG motifs affects both dimerization and the Aβ processing. However, as showed in Chapter I, I demonstrated that the GXXXG motifs in C99 are not critical in the substrate dimerization. This raised a question as to whether or not the motifs are involved in the processing of C99 to Aβ.

To test this, I investigated the effects of amino acid substitutions in the GXXXG motifs on Aβ production in an *in vitro* assay system using 3-[(3-cholamidopropyl) dimethylammonio]-2-hydroxy-1-propanesulfonate (CHAPSO)-solubilized γ-secretase and C99 substrate. This assay system is suitable for this purpose because the genuine enzymatic activity can be assessed in the *in vitro* assay without being interfered by other factors such as their subcellular

localizations. CHAPSO is a zwitterionic surfactant used to solubilize biological macromolecules such as proteins. Cladera and colleagues reported that CHAPSO and a similar detergent CHAPS (3-[(3-cholamidopropyl)dimethylammonio]-1-propanesulfonate) are especially useful non-denaturing detergents in purifying membrane proteins, which often exhibit very low or no solubility in aqueous solution due to their hydrophobicity (Cladera *et al.* 1997). Using this detergent, solubilized γ-secretase assay systems have been established and reported (Kakuda *et al.* 2006; Li *et al.* 2000; Fraering *et al.* 2004). The most striking feature of this type of assay system is its highly specific activity of γ-secretase. Also, it replicates the ratio of Aβ42 over the total Aβ generated observed in cellular assay systems (Asami-Odaka *et al.* 1995; Li *et al.* 2000), showing the suitability of these *in vitro* assay systems to investigate γ-secretase activity.

In this study, I used the assay system reported by Kakuda and colleagues, as the apparent V_{max} values of Aβ and AICD in this system were roughly more than 30-fold higher than those in similar systems (Fraering *et al.* 2004; Hayashi *et al.* 2004). Furthermore, not only Aβ40 and Aβ42, but also their precursor species such as Aβ45, Aβ48, and Aβ49 can be detected and quantified (Kakuda *et al.* 2006), such that I can investigate how Aβ processing is regulated by the GXXXG motifs in very details. Using this assay combined with mass spectrometry, I demonstrate that the GXXXG motifs are involved in the regulation of the successive processing of Aβ by γ-secretase.

Materials and Methods

Antibodies

The following antibodies were used in this study: anti-human Aβ antibody 82E1 (IBL); anti-human Aβ antibody 4G8 (Covance); ANTI-FLAG® M2 antibody (Sigma−Aldrich), anti-nicastrin antibody N1660 (Sigma−Aldrich); anti-presenilin 1-carboxyl-terminal fragment (CTF) antiserum (a gift from Drs. T. Tomita and T. Iwatsubo, The University of Tokyo); anti-Pen-2 antibody (a gift from Dr. A. Takashima, The University of Gakushuin); and anti-Aph-1a loop antibody O2F1 (Covance). The detail of 82E1 is described in Chapter I (see Fig. 1-2). 4G8 is reactive to the amino acid residues Aβ17−24 (LVFFAEDV). The epitope lies within Aβ18−22 (VFFAE) (Fig. 2-1). ANTI-FLAG® M2 antibody recognizes the FLAG peptide sequence (DYKDDDDK). Anti-nicastrin antibody N1660 was raised against a synthetic peptide corresponding to the carboxyl terminus of human nicastrin (amino acids 693−709; KADVLFIAPREPGAVSY) conjugated to keyhole limpet hemocyanin as an immunogen.

Preparation of C99-FLAG Substrates

Preparation of C99-FLAG substrates was performed as described in detail in Chapter Ⅰ.

Preparation of CHAPSO-Solubilized γ-Secretase

Preparation of CHAPSO-solubilized γ-secretase was performed as described previously (Kakuda *et al.* 2006). In detail, the harvested N2a or mouse embryonic fibroblast cells were homogenized in Homogenizing Buffer [20 mM piperazine-N, N′-bis (2-ethanesulfonic acid) (PIPES), pH 7.0, 140 mM KCl, 0.25 M sucrose, 5 mM ethylene glycol tetraacetic acid (EGTA)] using a glass/Teflon homogenizer. The homogenates were centrifuged at 1,000 ×*g* and 4°C for 10 min to remove nuclei and large cell debris. The postnuclear supernatants were recentrifuged at 100,000 ×*g* and 4°C for 1 h. The resulting pellets representing the microsomal fractions were suspended in a buffer (50 mM PIPES, pH 7.0, 0.25 M sucrose, 1 mM EGTA). Their protein concentrations were adjusted to 10 mg/ml. The membranes were solubilized by the addition of an equal volume of 2×NK buffer [50 mM PIPES, pH 7.0, 0.25 M sucrose, 1 mM EGTA, 2% CHAPSO (Sigma−Aldrich), 2 mM diisopropyl fluorophosphate, 20 μg/ml antipain, 20 μg/ml leupeptin, 20 μg/ml 1-chloro-3-tosylamido-7-amino-2-heptanone (TLCK), 10 mM phenanthroline, and 2 mM thiorphan] and incubated at 4°C for 45 min. After centrifugation at 100,000 ×*g* and 4°C for 1 h, the supernatants were collected (1% CHAPSO lysate).

Aβ and AICD Detection by CHAPSO-Solubilized γ-Secretase Assay System

The procedure of the CHAPSO-solubilized γ-secretase assay system was as follows: 1% CHAPSO lysate was diluted with 2.27 volumes of CHAPSO-free buffer (50 mM PIPES, pH 7.0, 0.25 M sucrose, 1 mM EGTA, 1 mM diisopropyl fluorophosphate, 10 μg/ml antipain, 10 μg/ml leupeptin, 10 μg/ml TLCK, 5 mM phenanthroline, and 1 mM thiorphan) containing defined amounts of C99-FLAG. Furthermore, 1% phosphatidylcholine (solubilized in 1% CHAPSO) (Sigma−Aldrich) was added to the diluted lysate, which significantly enhanced the activity of γ-secretase but did not alter the ratio of Aβ42/Aβ40 produced. Before starting the reaction, the residual Nonidet-P 40 in the substrate must be evaluated carefully (Kakuda *et al.* 2006). A Nonidet-P 40 concentration of 0.05% or more should be avoided because this would decrease γ-secretase activity. In this study, I maintained the final Nonidet-P 40 concentration at 0.045%. The reaction mixture was incubated at 37°C for 4 h. The samples were separated on 12% Tris−Tricine SDS-containing gels by SDS-PAGE. Gels were transferred onto a nitrocellulose membrane (0.2 μm pore size) (GE Healthcare). The subsequent procedure was as described in detail in Chapter Ⅰ. 82E1 antibody was utilized to detect Aβ and ANTI-FLAG® M2 antibody was used to detect AICD.

Matrix-Assisted Laser Desorption/Ionization Time-Of-Flight Mass Spectrometry （MALDI-TOF-MS） Analysis

To measure the relative levels of different Aβ species, I employed the matrix-assisted laser desorption/ionization time-of-flight mass spectrometry (MALDI-TOF MS), which has been used in previous studies (Kakuda *et al.* 2006; Okochi *et al.* 2013). The MALDI-TOF-MS analysis procedure in this study was as follows. After incubating the samples in the CHAPSO-solubilized γ-secretase assay system with C99-FLAG as described above, 1/10 volume of 10% Nonidet-P 40 was added to stop the reaction between the substrate and γ-secretase. The mixture volume was scaled up 30-60 times scale compared with that for the Western blotting. The mixture was agitated with 25 μl of Protein G Sepharose beads (GE Healthcare) and 3 μl of ANTI-FLAG® M2 antibody (Sigma−Aldrich) at 4°C overnight to remove AICD. The suspension was centrifuged at 10,000 rpm and 4°C for 1 min. The supernatants were agitated with 25 μl of Protein G Sepharose beads (GE Healthcare) with 3 μl of 4G8 antibody at 4 °C overnight. The suspension was centrifuged at 10,000 rpm and 4°C for 1 min. After removing the supernatants, the beads were washed five times with 1 ml of Tris-buffered saline (TBS) (50 mM Tris-HCl, 150 mM NaCl, pH 7.6) and then three times with 1 ml of deionized water. After sufficient washing, the beads were dried at 30°C in a SpeedVac and eluted with a matrix composed of a mixture of 2.5% trifluoroacetate and 50% acetonitrile containing α-cyano-4-hydroxycinnamic acid (CHCA) incubated at 37°C for 30 min. The masses of

the peptides were defined using a matrix-assisted laser desorption/ionization time-of-flight mass spectrometer (MALDI-TOF-MS), using a 4800 Plus MALDI-TOF-TOF™ Analyzer (AB Sciex). Aβ species were determined by their theoretical masses.

Coimmunoprecipitation of C99-FLAG Substrates

Coimmunoprecipitation of C99-FLAG substrates was conducted as described previously (Funamoto *et al.* 2013). Briefly, 50 µl of C99-FLAG substrates were immobilized on 15 µl of ANTI-FLAG® M2 Magnetic Beads (Sigma−Aldrich) by incubating them together at 4°C for 2 h. After incubation, the suspension was spun down and the supernatant was removed. Next, the beads were washed once with 500 µl of PBS containing 1% of Nonidet-P 40 and five times with 750 µl of 0.25% CHAPSO buffer (50 mM PIPES, pH 7.0, 0.25 M sucrose, 1 mM EGTA, 0.25% CHAPSO). After washing, the beads were incubated with CHAPSO-solubilized γ-secretase at 4°C overnight. After incubation, the suspension was spun down and the supernatant was removed. Next, the beads were washed five times with 750 µl of 0.25% CHAPSO buffer. After washing the coimmunoprecipitates, samples were subjected to Western blotting to detect presenilin 1-CTF, the potential catalytic subunit of γ-secretase.

Statistical Analysis

Band intensity was quantified using a LAS-4000 luminescent image analyzer (Fujifilm). Holm−Sidak's post hoc test was used for comparison of the C99 mutants with that of WT. All data are shown as mean ± standard error of the mean (SEM), and statistical significance was assessed at $p < 0.05$.

Results

To gain insights into how the amino acid substitutions in the GXXXG motifs influence the γ-secretase processing of C99, I performed the CHAPSO-solubilized γ-secretase assay, which allows rather free collisions between enzymes and substrates in a soluble state (Kakuda *et al.* 2006). Surprisingly, Aβ production from 1G and 0G (A) after 4 h incubation was significantly decreased compared to that from WT, suggesting that 1G and 0G (A) mutants are inefficient substrates of γ-secretase (Fig. 2-2). The levels of AICD, the counterpart of Aβ, also decreased in those mutants (Fig. 2-3). I further analyzed the total Aβ produced from the 0G (L) and 0G (F) mutants. Aβ production from 0G (L) and 0G (F) appeared higher than that from 0G (A), and Aβ production from 0G (F) was significantly increased compared to that from WT (Fig. 2-4). Since I modified the amino acid sequence of the substrate, it is possible that Aβ, or Aβ-like peptides, is produced by other proteases from the cells, from which γ-secretase was extracted, with the C99 mutants. To rule out this possibility, I examined whether a specific γ-secretase inhibitor, N-[N-(3,5-difluorophenacetyl)-L-alanyl]-S-phenylglycine t-butyl ester (DAPT), affects the production of Aβ from the mutants (Dovey *et al.* 2001). DAPT suppressed Aβ production with all mutants (Fig. 2-5; Kakuda *et al.* 2006; Takami *et al.* 2009), indicating that they are all processed by γ-secretase.

It is also possible that the amino acid substitutions reduce the binding of 1G and 0G (A)

to the enzyme, thereby reducing the production of Aβ. To examine whether γ-secretase fails to recognize these mutants, I immunoprecipitated the C99-FLAG substrates and quantified the levels of the carboxyl-terminal fragment of PS1, which is a major component and the potential catalytic subunit of γ-secretase (Funamoto *et al.* 2013). It has been reported that PS1 undergoes auto-endoproteolysis between transmembrane domain 6 and transmembrane domain 7 to generate ～16-17 kDa carboxyl- and ～27-28 kDa amino-terminal fragments, which reflect the active state of the γ-secretase (Thinakaran *et al.* 1996). As described in Materials and Methods, the coimmunoprecipitates were prepared at 4℃ to suppress the cleavage activity of the γ-secretase. I was able to detect substantial binding of PS1-CTF to C99 WT as well as 3G, 2G, 0G (L), and 0G (F) (Fig. 2-6A and B), which is consistent with the robust Aβ production from these substrates (Figs. 2-2 and 2-4). Interestingly, 1G and 0G (A) also showed substantial interactions with PS1-CTF (Fig. 2-6A). There was no significant difference in the levels of PS1-CTF coimmunoprecipitation among all substrates (Fig. 2-6C). These findings suggest that substitutions at GXXXG motifs affect the efficiency of cleavage by γ-secretase rather than interaction with the enzyme.

From a therapeutic perspective, it is important to understand not only how much and fast Aβ is produced but also how C99 is processed to produce amyloidogenic Aβ. Therefore, I examined the effects of amino acid substitutions in the GXXXG motif on the production of Aβ species in the solubilized γ-secretase assay using MALDI-TOF-MS. As described earlier, it is

currently considered that there are two production lines of Aβ to produce either Aβ40 or Aβ42 from their longer precursor species, Aβ49 and Aβ48, respectively. As the result of the successive processing, it is expected that Aβ34, Aβ37, Aβ38, Aβ43, and Aβ45 are detected in addition to Aβ40 and Aβ42. Using the high sensitive MS, I was able to detect Aβ34, Aβ38, Aβ40, Aβ42, and Aβ43 and compared their relative abundance with each substrate (Fig. 2-7A). Surprisingly, the levels of the amyloidogenic Aβ42 and Aβ43 were dramatically reduced with all C99 Ala mutants (Fig. 2-7A and B). There was also concomitant increase of Aβ40, Aβ38, and Aβ34, albeit not significant except for Aβ34 for 3G and 2G (Fig. 2-7A and B). These results indicate that Aβ42 and Aβ43 are processed further to produce shorter Aβ species with the mutations in the GXXXG motifs. To investigate this, I also compared the ratios of precursor/product, Aβ42/Aβ38 and Aβ43/Aβ40. It has been reported that the ratios of Aβ38/Aβ42 and Aβ40/Aβ43 increase in cerebrospinal fluid (CSF) from patients with mild cognitive impairment (MCI)/AD. That is to say, the γ-secretase cleavage in MCI/AD patients shifted toward the amino terminus (Kakuda *et al.* 2012, 2013; Chávez-Gutiérrez *et al.* 2012). It should be noted that I used inversed ratios in my study to avoid zero in the denominator. Surprisingly, these ratios were significantly decreased with the Ala mutants (Fig. 2-7C and D), suggesting that the successive processing of C99 is facilitated to generate shorter Aβ species from the longer amyloidogenic Aβ42 and Aβ43. This shift of Aβ processing was even more pronounced with 0G (L) and 0G (F) mutants. In fact, there was almost no

Aβ42 and Aβ43 detected, whereas the short Aβ production was greatly enhanced (Fig. 2-8A and B). In addition, the ratios of precursor/product were significantly decreased in those mutants (Fig. 2-8C and D).

Moreover, there is a relationship between a ratio of produced Aβ species and age onset of the disease in different families (De Jonghe *et al.* 2001). In detail, when the ratio of Aβ42/Aβ40 in familial AD mutations near the γ-secretase cleavage site of APP is compared with that in WT APP, the ratio increased in the mutations (De Jonghe *et al.* 2001). In addition, as the ratio of Aβ42/Aβ40 increased, the age onset of the disease became younger (De Jonghe *et al.* 2001). In reference to this, I analyzed the ratio of Aβ42/Aβ40, and showed that it decreased for all mutants (Figs. 2-7E and 2-8E). These results indicate that the GXXXG motifs are important in regulating the progressive processing of C99 by γ-secretase.

Discussion

It is widely accepted that Aβ48 and Aβ49 are first generated from C99, by a process called ε-cleavage, by γ-secretase. These long precursor species are then successively cleaved by the same enzyme by three to four residues at a time to generate shorter Aβ species. This results in two separate lines of products from Aβ48 and Aβ49. Aβ48 is processed to Aβ45, Aβ42, and Aβ38, whereas Aβ49 is processed to Aβ46, Aβ43, Aβ40, Aβ37, and Aβ34 with Aβ40 and Aβ42 being the major species produced. Among them, Aβ42 and Aβ43 are most amyloidogenic, such that the mechanisms regulating the generation of these species are of great interest in the field of Alzheimer neuropathology (Iwatsubo *et al.* 1994; Younkin 1995; Saito *et al.* 2011). In this thesis study, I investigated how the GXXXG motifs in C99 affects this γ-cleavage and found that mutating the GXXXG motifs generally result in the reduction of Aβ42 and Aβ43 and augmentation of shorter Aβ species (e.g., Aβ34) (Figs. 2-7A, B, 2-8A, and B). These results indicate that the GXXXG motifs determine the processing propensity at each γ-cleavage site. I will discuss how these modifications may cause the altered processing in details in General Discussion.

In this study, I was unable to detect Aβ48 and Aβ49 as well as Aβ45 and Aβ46 (Figs. 2-7A and 2-8A). It was not possible to identify long Aβ species by MALDI-TOF-MS, presumably due to their hydrophobicity. However, it has been reported that Aβ species longer than Aβ45 were detected by not MALDI-TOF-MS but in Urea-PAGE in CHAPSO-solubilized γ-secretase assay

system (Kakuda *et al.* 2006). Therefore, there is a possibility that Aβ species longer than Aβ45 from the GXXXG mutations were produced but not detected in my experiments.

Figures

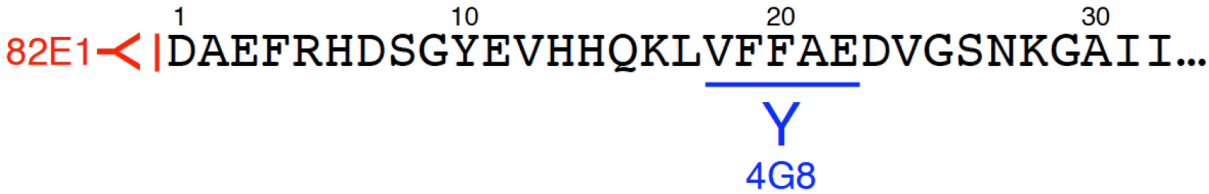

Figure 2-1. Immunoactivity of anti-Aβ antibodies. Recognition sites of anti-Aβ antibodies in the human C99/Aβ sequence. The number represents Aβ numbering. 82E1 is specific to the amino-terminal end of human Aβ. Therefore, it is very useful to detect APP fragments generated by β-secretase cleavage. The specificity of 4G8 is Aβ18−22 (VFFAE). It reacts to the abnormally processed Aβ isoforms (e.g., Aβ38, Aβ40, Aβ42, and Aβ43) as well as precursor forms (i.e., APP and C99).

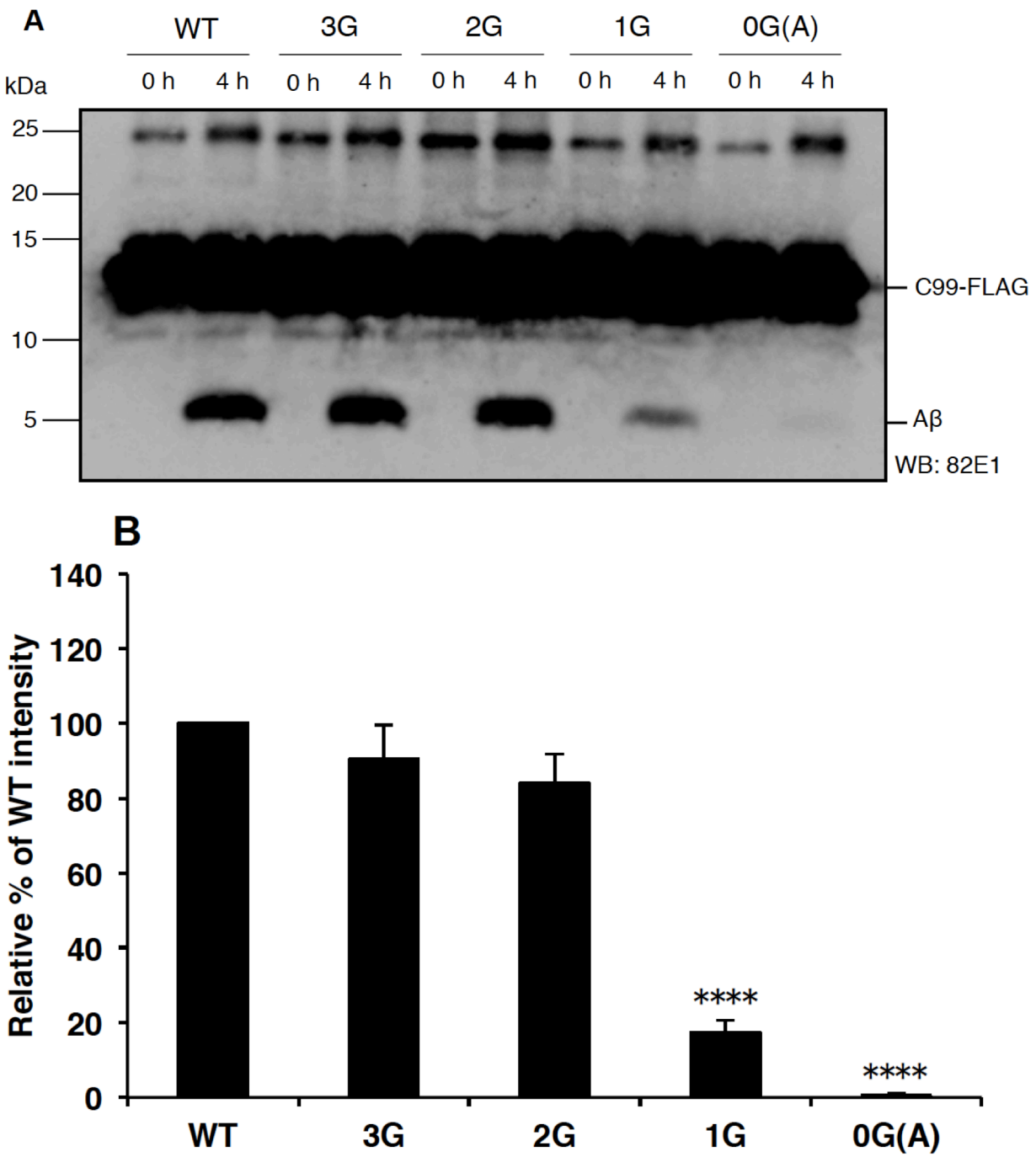

Figure 2-2. Effects of alanine substitution on Aβ production in the CHAPSO-solubilized γ-secretase assay system. (A) CHAPSO-solubilized γ-secretase reaction solutions containing each substrate were subjected to Western blotting with 82E1 antibody to detect Aβ. γ-Secretase prepared from Neuro2a cells was used. Reaction times were 0 and 4 h. Aβ production from 1G and 0G (A) was significantly decreased. (B) The band intensity of Aβ was measured using a LAS-4000 luminescent image analyzer. Band intensity of Aβ in WT was set at 100%. Aβ production from 1G and 0G (A) was significantly reduced compared with that in WT, suggesting that 1G and 0G (A) mutants are inefficient substrates of γ-secretase. Data are expressed as mean ± SEM (n = 5, ****: $p < 0.001$, ANOVA with Holm−Sidak's post hoc test compared with WT).

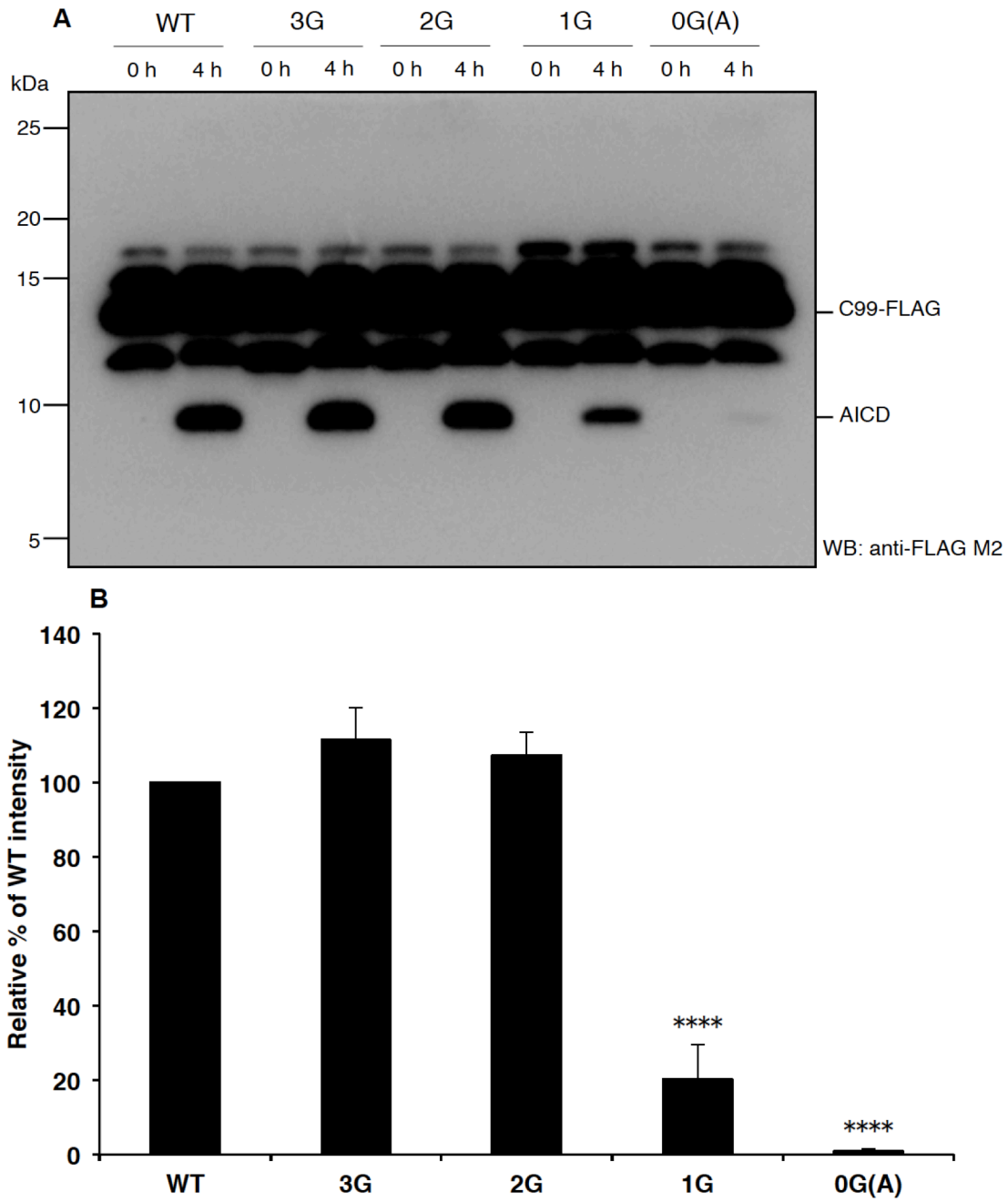

Figure 2-3. Effects of alanine substitution on AICD production in the CHAPSO-solubilized γ-secretase assay system. (A) CHAPSO-solubilized γ-secretase reaction solutions containing each substrate were subjected to Western blotting with ANTI-FLAG® M2 antibody to detect AICD. γ-Secretase prepared from Neuro2a cells was used. Reaction times were 0 and 4 h. AICD production from 1G and 0G (A) was significantly decreased. The result of AICD production is similar to that for Aβ (see Fig. 2-2). (B) The band intensity of AICD was measured using a LAS-4000 luminescent image analyzer. Band intensity of AICD in WT was set at 100%. AICD production from 1G and 0G (A) was significantly reduced compared with that in WT, suggesting that 1G and 0G (A) mutants are inefficient substrates of γ-secretase. Data are expressed as mean ± SEM (n = 3, ****: $p < 0.001$, ANOVA with Holm−Sidak's post hoc test compared with WT).

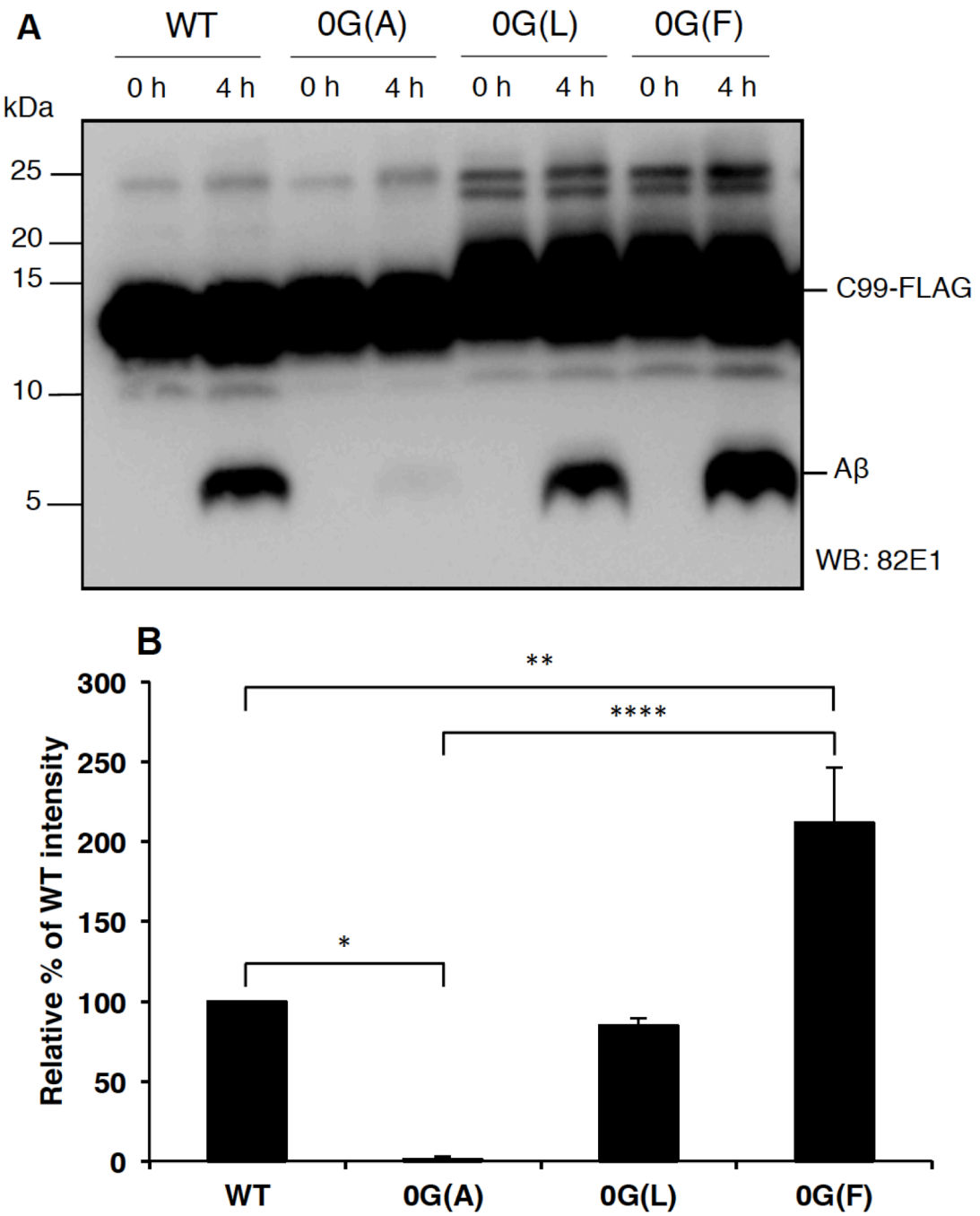

Figure 2-4. Effects of substitution in the motif of C99 on Aβ production in the CHAPSO-solubilized γ-secretase assay system. (A) CHAPSO-solubilized γ-secretase reaction solutions containing WT, 0G (A), 0G (L), and 0G (F) were subjected to Western blotting with 82E1 antibody to detect Aβ. γ-Secretase prepared from mouse embryonic fibroblast (MEF) cells was used. Reaction times were 0 and 4 h. (B) The band intensity of Aβ was measured using a LAS-4000 luminescent image analyzer. Band intensity of Aβ in WT was set at 100%. Aβ production from 0G (L) and 0G (F) tended to increase compared with that in 0G (A), and Aβ production from 0G (F) increased compared with that in WT. Data are expressed as mean ± SEM (n = 3, *: $p < 0.05$; **: $p < 0.01$; ****: $p < 0.001$, ANOVA with Holm−Sidak's post hoc test compared with WT).

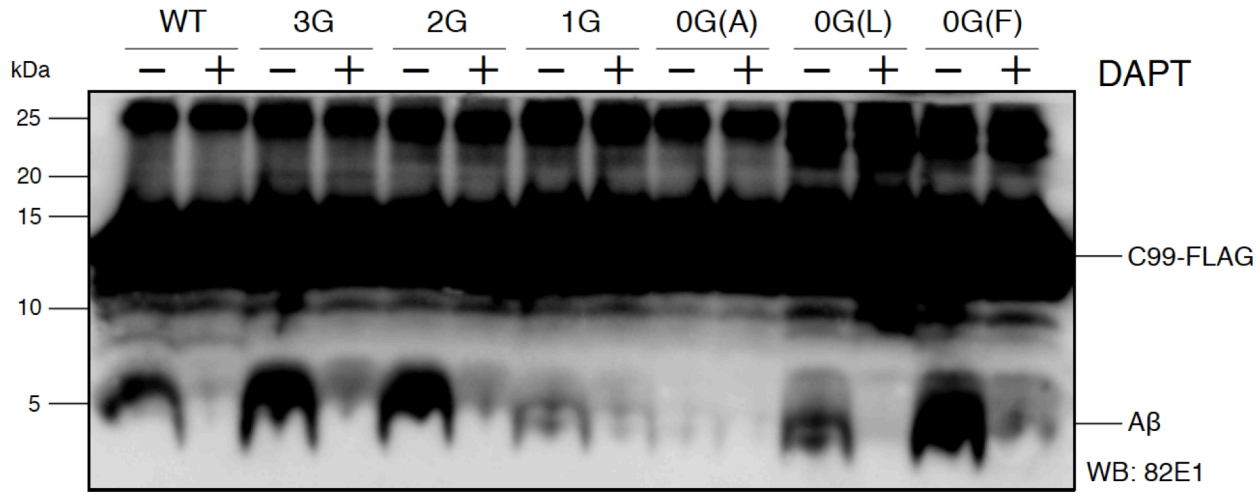

Figure 2-5. Effects of γ-secretase inhibitor in the CHAPSO-solubilized γ-secretase assay system. CHAPSO-solubilized γ-secretase reaction solutions containing each substrate and γ-secretase inhibitor, N-[N-(3,5-difluorophenacetyl)-L-alanyl]-S-phenylglycine t-butyl ester (DAPT) were subjected to Western blotting with 82E1 antibody to detect Aβ. The final concentration of DAPT is 1 μM. Reaction time was 4 h. − indicates without inhibitor and + indicates with inhibitor. DAPT suppressed Aβ production.

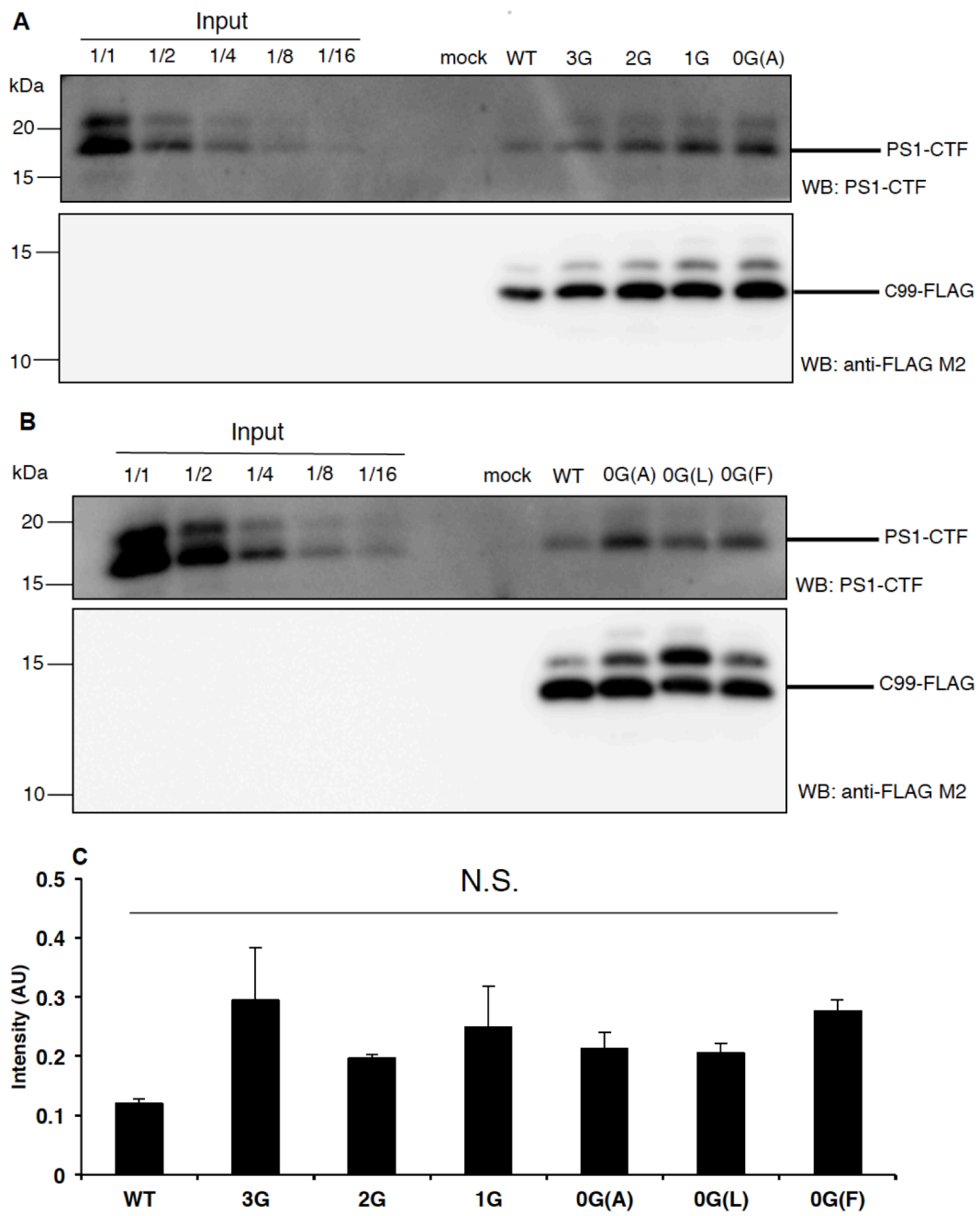

Figure 2-6. Coimmunoprecipitation of C99-FLAG substrates. (A and B) C99-FLAG substrates were immobilized on ANTI-FLAG® M2 magnetic beads and incubated with CHAPSO-solubilized γ-secretase. γ-Secretase prepared from Neuro2a cells was used. After sufficient washing of the coimmunoprecipitates, samples were subjected to Western blotting to detect and quantify presenilin 1 carboxyl terminal fragment (PS1-CTF) and C99. (C) Quantitative analysis of interacted PS1-CTF. The intensities of PS1-CTF and C99 were measured using a LAS 4000 luminescent image analyzer. The ratio of PS1-CTF/C99 was calculated. 1G and 0G (A) showed distinct interactions with the PS1-CTF. In addition, 0G (A), 0G (L), and 0G (F) showed no significant alteration from WT in their interaction with PS1-CTF. Data are expressed as mean ± SEM (n = 3–6, ANOVA with Holm–Sidak's post hoc test compared with WT). N.S. indicates not significant.

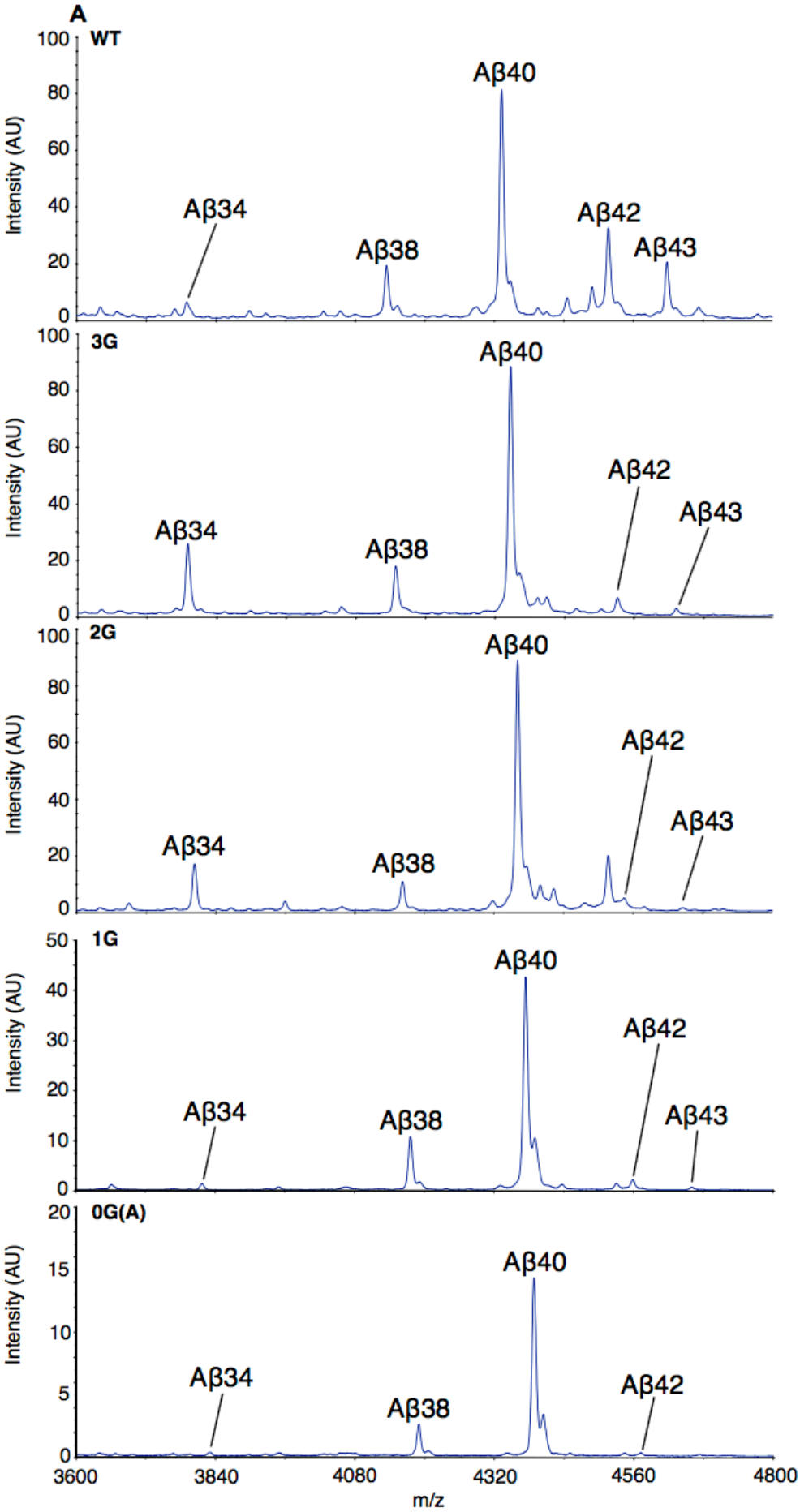
A
WT
3G
2G
1G
0G(A)
Intensity (AU)
Aβ34
Aβ38
Aβ40
Aβ42
Aβ43
m/z
3600
3840
4080
4320
4560
4800

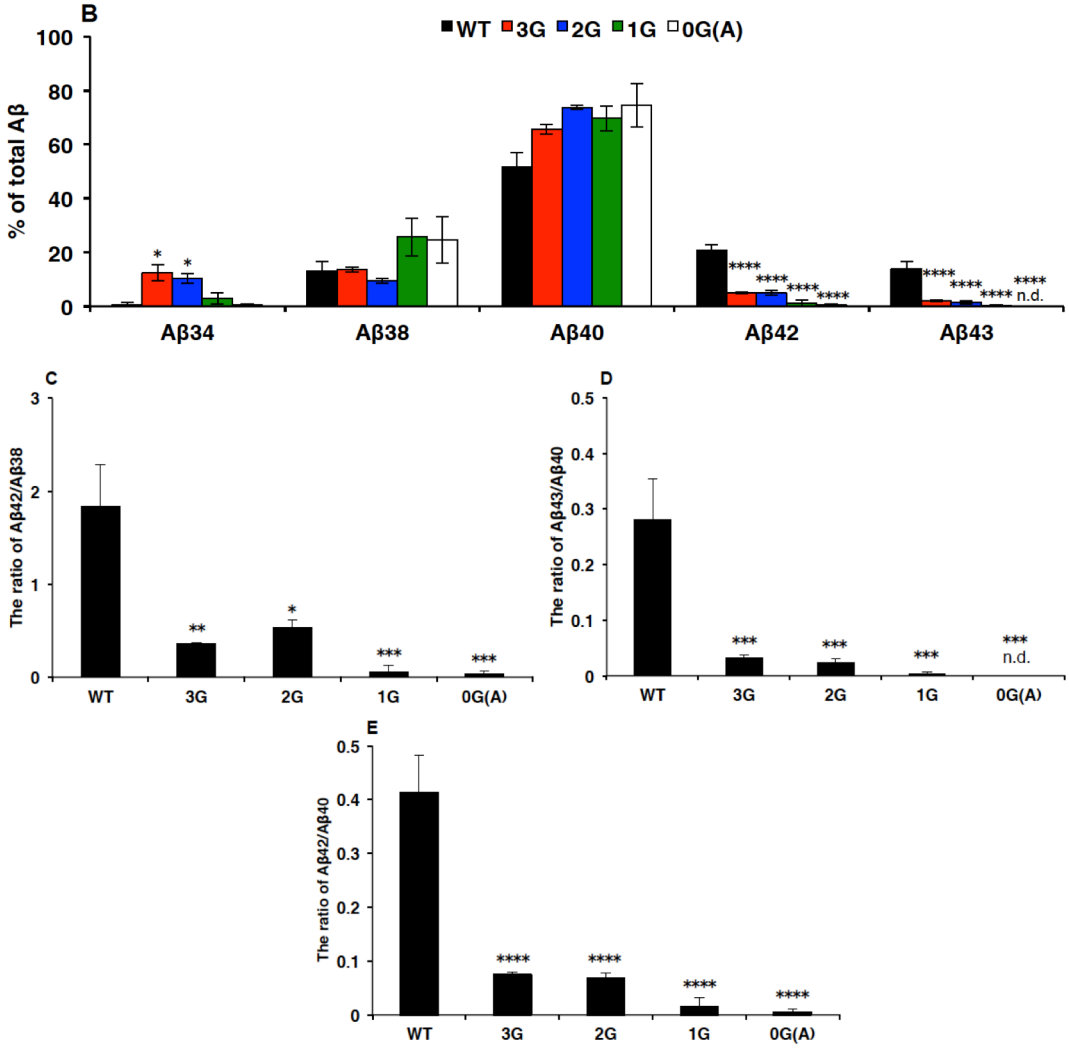

Figure 2-7. Production of Aβ species modulated by alanine substitution in the CHAPSO-solubilized γ-secretase assay system. (A) Production of Aβ species modulated by alanine substitution. Total Aβ produced from CHAPSO-solubilized γ-secretase assay system was immunoprecipitated with 4G8 antibody and subjected to MALDI-TOF-MS. γ-Secretase prepared from Neuro2a cells was used. (B) Percentage of Aβ species from each C99-FLAG substrate was calculated by MS using peak intensity. The sum of all peak intensities was set as 100%, and the percentage of each Aβ species was calculated. Percentages of Aβ42 and Aβ43 decreased for all mutants, and 1G and 0G (A) showed a trend to a concomitant increase of Aβ38 and Aβ40 production. In addition, the production of short Aβ species (e.g., Aβ34) was elevated for 3G and 2G. (C and D) Ratios of Aβ42/Aβ38 and Aβ43/Aβ40, which indicate the ratios of precursor/product, respectively. I calculated these ratios using the percentage of each Aβ species calculated in (B). These ratios decreased for all mutants. (E) Ratio of Aβ42/Aβ40. I calculated the ratio using the percentage of each Aβ species calculated in (B). The ratio decreased for all mutants. Data are expressed as mean ± SEM (n = 3–4, *: $p < 0.05$; **: $p < 0.01$; ***: $p < 0.005$; ****: $p < 0.001$, ANOVA with Holm–Sidak's post hoc test compared with WT). n.d. indicates not detected.

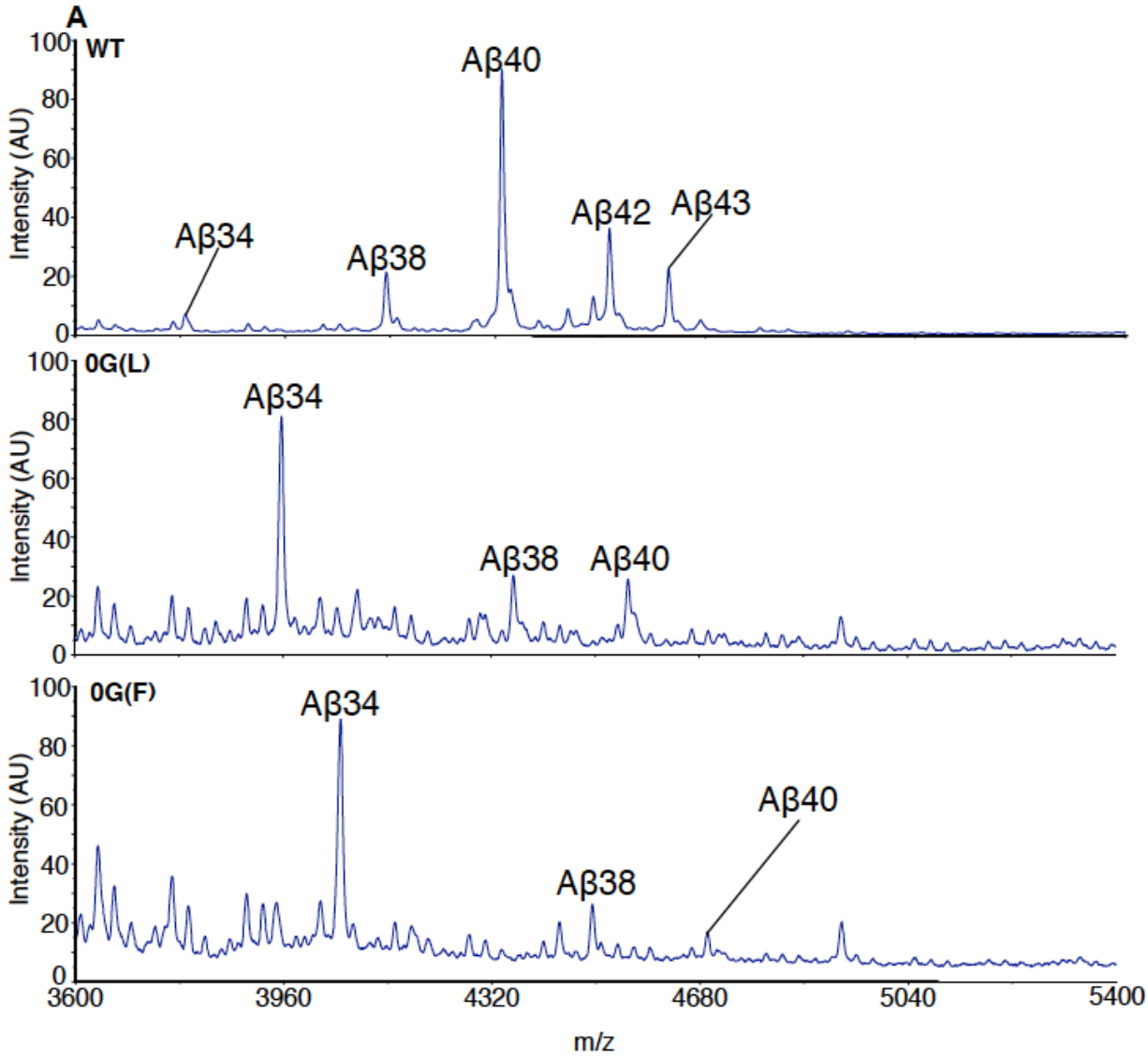
A
WT
Aβ40
Aβ34
Aβ38
Aβ42
Aβ43
0G(L)
Aβ34
Aβ38
Aβ40
0G(F)
Aβ34
Aβ40
Aβ38
Intensity (AU)
100
80
60
40
20
0
3600
3960
4320
4680
5040
5400
m/z

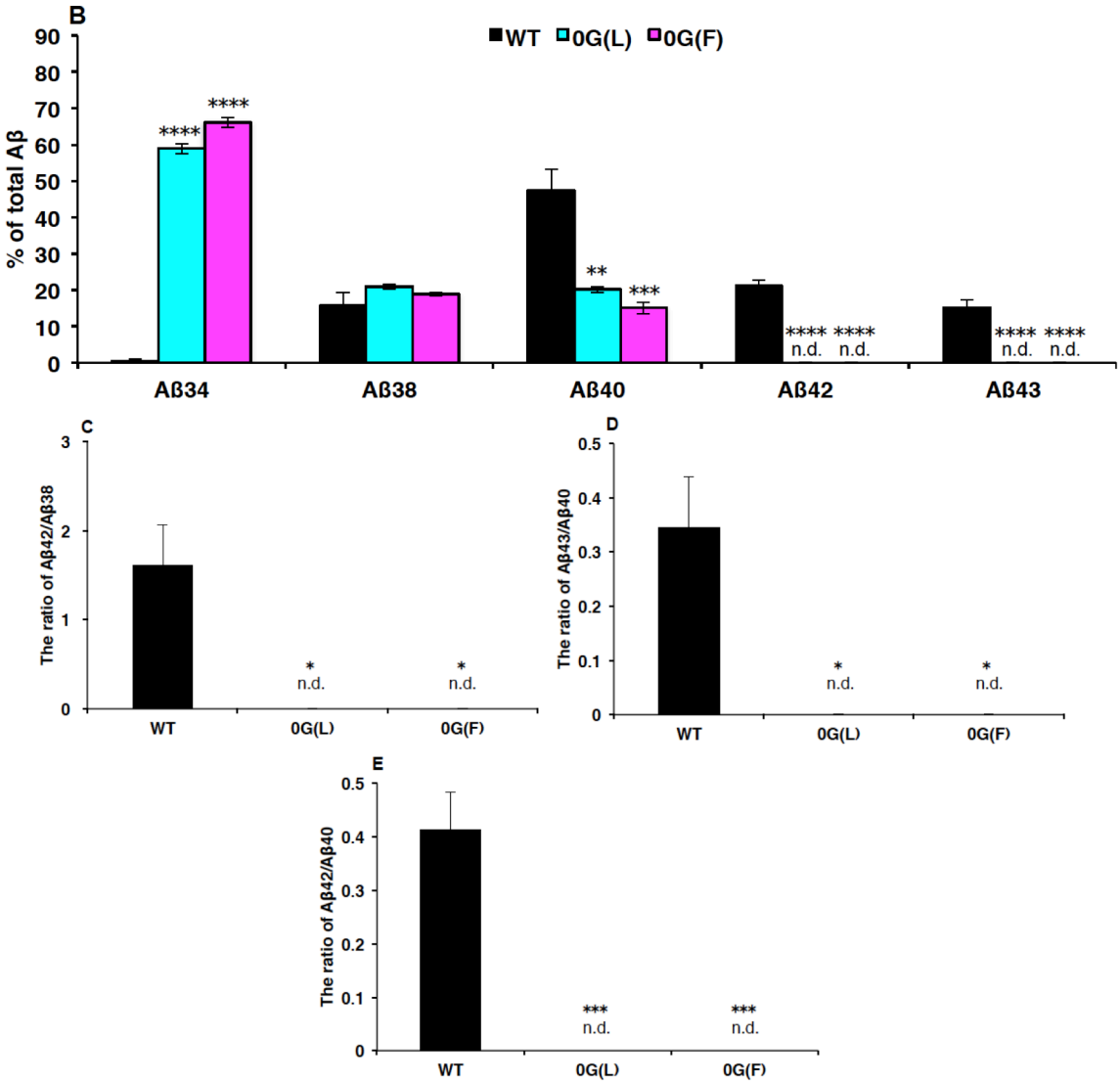

Figure 2-8. Production of Aβ species modulated by substitution in the CHAPSO-solubilized γ-secretase assay system. (A) Production of Aβ species modulated by leucine or phenylalanine substitution. Total Aβ produced from CHAPSO-solubilized γ-secretase assay system was immunoprecipitated with 4G8 antibody and subjected to MALDI-TOF-MS. γ-Secretase prepared from Neuro2a cells was used. (B) Percentage of Aβ species from each C99-FLAG substrate was calculated by MS using peak intensity. The sum of all peak intensities was set as 100%, and the percentage of each Aβ species was calculated. Percentages of Aβ40, Aβ42, and Aβ43 decreased for all mutants, and production of short Aβ species (e.g., Aβ34) was elevated for those mutants. (C and D) Ratios of Aβ42/Aβ38 and Aβ43/Aβ40, which indicate the ratios of precursor/product, respectively. I calculated the ratios of Aβ42/Aβ38 and Aβ43/Aβ40 using the percentage of each Aβ species calculated in (B). These ratios decreased for all mutants. (E) Ratio of Aβ42/Aβ40. I calculated the ratio using the percentage of each Aβ species calculated in (B). The ratio decreased for all mutants. Data are expressed as mean ± SEM (n = 3–4, *: $p < 0.05$; **: $p < 0.01$; ***: $p < 0.005$; ****: $p < 0.001$, ANOVA with Holm−Sidak's post hoc test compared with WT). n.d. indicates not detected.

Chapter Ⅲ.

Analyses of substitution in GXXXG motifs on C99 dimerization and on γ-cleavage in living cells

Introduction

I showed the following findings in the solubilized γ-secretase assay. (1) Substitutions in the GXXXG motif failed to alter C99 dimerization in a detergent-soluble state (Fig. 1-4). (2) Aβ production from 1G and 0G (A) was significantly decreased compared with that from WT, suggesting that 1G and 0G (A) mutants are inefficient substrates of γ-secretase (Fig. 2-2), although 1G and 0G (A) showed preserved interactions with the presenilin 1 CTF (PS1-CTF) (Fig. 2-6A and C). (3) Analysis of Aβ species using the MALDI-TOF-MS showed that the percentages of Aβ42 and Aβ43 decreased for all mutants with a trend of concomitant increases in shorter Aβ species (e.g., Aβ34) (Figs. 2-7A, B, 2-8A, and B). (4) As a consequence, the ratios of Aβ precursor/product decreased for all mutants (Figs. 2-7C, D, 2-8C, and D). (5) The ratio of Aβ42/Aβ40 decreased for all mutants (Figs. 2-7E and 2-8E). These results indicate that the GXXXG motifs in C99 are important in the successive processing by γ-secretase but not its dimerization. To extend these findings obtained in the *in vitro* assays to living cells, I studied the effect of the same mutations on the substrate dimerization and Aβ processing in Chinese Hamster Ovary (CHO) cells, which have been widely used as a model system for studying APP processing.

Materials and Methods

Antibodies

The following antibodies were used in this study: anti-human Aβ antibody 82E1 (IBL); and anti-human Aβ antibody 4G8 (Covance). The detail is described in Chapter Ⅱ.

DNA Oligonucleotides

The oligonucleotides to generate C99 mutants used in this study were shown in Table 1. See also Chapter Ⅰ.

DNA Constructs

Funamoto and colleagues constructed a plasmid DNA to express C99 in cells (Funamoto *et al.* 2004). The preparation procedure was as follows: Mammalian expression vector pcDNA3.1 containing APP751 was amplified by polymerase chain reaction (PCR) using the primers 5'-GAT GCA GAT GCA GAA TTC CGA CAT GAC TCA-3' and 5'-CGC CCG AGC CGT CCA GGC GGC CAG-3' and subjected to self-ligation to fuse the C99 coding sequence with the signal peptide (MLPGLALLLLAAWTARA) of APP. The resultant construct contained additional aspartic acid and alanine residues on the amino-terminal side of the β-cleavage site and is referred to here as DA-C99. This insertion allows the product to be cleaved by signal peptidase exactly at the

β-cleavage site, producing Aβ that starts from the first residue aspartic acid (Lichtenthaler *et al.* 1999a). For alanine substitution in the GXXXG motif of C99, I performed site-directed mutagenesis on the DA-C99 plasmid by PCR using the primers listed in Table 1. The C99 mutants were confirmed by DNA sequencing, using 3130xl Genetic Analyzers (Thermo Fisher Scientific). Resultant constructs were referred to here as 3G, 2G, 1G, and 0G (A).

Cell Culture and Transfection

CHO cells were cultured in Dulbecco's modified Eagle's medium (WAKO) supplemented with 10% fetal bovine serum (FBS) (Invitrogen) and penicillin/streptomycin (Invitrogen) at 37°C under humidified 5% CO_2 atmosphere. CHO cells were cultured in 12-well plates and transfected with 1 μg of pcDNA3.1 carrying WT, 3G, 2G, 1G, and 0G (A) (Fig. 1-1), using Lipofectamine® LTX & PLUS™ Reagent (Invitrogen), in accordance with the manufacturer's instructions. After 5 h of transfection, the culture media replaced with fresh media [Dulbecco's modified Eagle's medium (WAKO) supplemented with 10% FBS (Invitrogen)]. Forty-eight hours later, cells and conditioned media were collected and subjected to Western blotting, an analytical technique to detect specific proteins, to visualize and quantify the production of C99 and Aβ by 82E1 antibody.

SDS-PAGE Analysis

After transfection, cells were homogenized with Sample Buffer (1×) (2% SDS, 80 mM Tris-HCl, pH 6.8, 10% glycerol, 1% 2-Mercaptoethanol, and a slight amount of Phenol Red), and conditioned media were collected and centrifuged at 15,000 rpm and 4°C for 10 min. After centrifuging, the supernatants were collected. The procedure of SDS-PAGE is described in detail in Chapter Ⅰ.

Blue Native PAGE Analysis

After transfection, the samples for BN-PAGE were prepared, in accordance with the manufacturer's instruction. In detail, cells were homogenized with NativePAGE™ Sample Buffer (4×) and 1/10 volume of 10% DDM (Invitrogen) in PBS (137 mM NaCl, 2.7 mM KCl, 8.1 mM Na_2HPO_4, and 1.47 mM KH_2PO_4). The suspension was ultracentrifuged at 100,000 ×*g* and 4°C for 15 min. The supernatant was collected and then mixed with NativePAGE™ Sample Buffer (4×) (Invitrogen) and 1/5 volume of NativePAGE™ 5% G-250 Sample Additive (Invitrogen). The procedure of BN-PAGE is described in detail in Chapter Ⅰ.

Matrix-Assisted Laser Desorption/Ionization Time-Of-Flight Mass Spectrometry （MALDI-TOF-MS） Analysis

After transfection, a 1/10 volume of 10% Nonidet-P 40 was added to each collected conditioned medium. The procedure of MALDI-TOF-MS is described in detail in Chapter Ⅱ.

Statistical Analysis

Band intensity was quantified using a LAS-4000 luminescent image analyzer (Fujifilm). Holm−Sidak's post hoc test was used for comparison of the C99 mutants with that of WT. All data are shown as mean ± standard error of the mean (SEM), and statistical significance was assessed at $p < 0.05$.

Results

WT, 3G, 2G, 1G, and 0G (A) constructs were introduced into CHO cells to examine the effect of substitutions on the substrate dimerization in living cells. Lysates of transfected cells were subjected to BN-PAGE followed by immunochemical detection (Fig. 3-1). Despite extensive efforts, I failed to detect discrete multimeric and monomeric bands of C99 substrate in cell lysates, although monomeric C99 was readily detectable in regular SDS-PAGE and Western blotting (Fig. 3-2A). The weak detergent (DDM) used for the BN-PAGE assay might not be sufficient to extract C99 from cell membranes.

To test whether alanine substitutions in the GXXXG motifs affect Aβ production in cells, I quantified the levels of secreted Aβ because most of Aβ produced is released into the culture medium. In the cellular assay, Aβ production was detectable with the 0G (A) mutant (Fig. 3-2A), which did not show any detectable Aβ in the *in vitro* assay (see Fig. 2-2). Although there was a slight but significant increase in the Aβ production with 1G, all mutants showed somewhat comparable levels of Aβ in the conditioned media (Fig. 3-2A and B). In addition, no significant differences were observed between any mutant and WT in the production of the intracellular Aβ (Fig. 3-2A and B).

To examine the effects of alanine substitutions in the GXXXG motif on the production of Aβ species, the total Aβ in conditioned media was analyzed using MALDI-TOF-MS. Although

Aβ43 was not detected in this cellular system, I was able to detect Aβ species from 0G (A), and Aβ37 and Aβ39 from all mutants, thereby complementing the *in vitro* assay (Fig. 3-3A).

The percentages of Aβ42 were significantly decreased for 2G, 1G, and 0G (A) with concomitant increases in the levels of Aβ38 and decreases in the Aβ42/Aβ38 ratios (Fig. 3-3A, B, and C). These results indicate that the processing of Aβ42 to Aβ38 is facilitated in these mutants including 0G (A), and are consistent with the results of 2G and 1G in the *in vitro* assay (see Fig. 2-7A, B, and C). These mutants also exhibited decreased levels of Aβ40 (Fig. 3-3B). However, the level of Aβ37, a putative product from Aβ40, was increase only for 0G (A) (Fig. 3-3B). The putative downstream product of Aβ37, Aβ34, was increased with all three mutants (Fig. 3-3B). In addition, the ratio of Aβ40/Aβ37 decreased only for 0G (A) (Fig. 3-3D). Therefore, the alanine substitutions in the GXXXG motifs shift the γ-secretase processing toward the amino terminal side. Moreover, the ratio of Aβ42/Aβ40 decreased only for 0G (A) (Fig. 3-3E). Taken together with the findings in the *in vitro* assay, these results suggest that the GXXXG motifs regulate the γ-cleavage site of C99.

Discussion

The overall effect of GXXXG mutations was consistent between the *in vitro* and cell-based assays, such that the mutations resulted in a decrease in long Aβ species and a concomitant increase in short Aβ species. Particularly, the reduction of amyloidogenic Aβ42 was remarkable in both assays. I will discuss how the mutation could cause these changes in details in General Discussion in the next chapter.

A big difference in the cell-based assay from the *in vitro* assay was the increased production of Aβ from 1G (Figs. 2-2, 3-2A, and B). Since my data from the coimmunoprecipitation assay indicated that 1G and 0G (A) can bind to γ-secretase (Fig. 2-6A), it might be possible that 1G is more concentrated in cellular structures with the enzyme and therefore given more time to be processed in cells. In fact, it is known that some mutations in APP result in altered localization of the precursor protein in cells (Martin *et al.* 1995; Kokawa *et al.* 2015). Alternatively, γ-secretase in CHO cells is more permissive to alterations in the GXXXG motif regarding the catalytic efficiency than the enzyme in N2a cells used for the *in vitro* assay.

In the cell lysate, putative SDS-resistant C99 dimer was detected (Fig. 3-2A), which might also have been present in the purified C99 in Chapter I. It has been reported that interactions via GXXXG motifs is tight and can be resistant to denaturing agents such as SDS

(Kienlen-Campard *et al.* 2008). Nevertheless, I observed no differences in the levels of these SDS-resistant dimers with the GXXXG mutants of C99 (Fig. 3-2A and C).

Figures

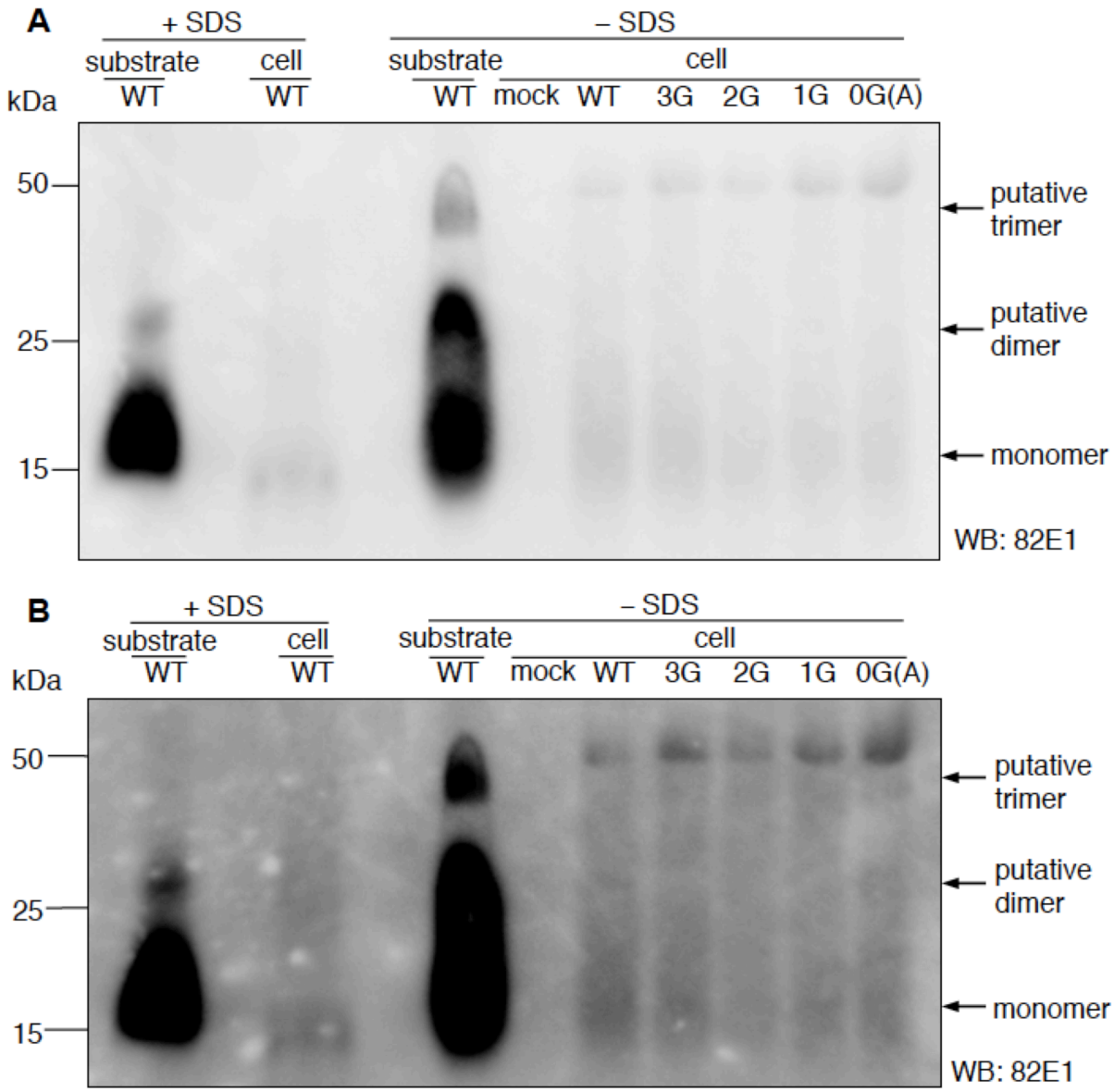

Figure 3-1. Analysis of substrate dimerization by BN-PAGE from cells. Lysates of transfected cell lysates were separated by blue native PAGE (BN-PAGE). Monomer, dimer, and trimer of the cell lysates were visualized using 82E1 antibody. Unfortunately, discrete multimeric and monomeric bands of C99 substrate in cells failed to be detected. WT substrate prepared from Sf9 cells and lysates of transfected cells from WT in the presence of SDS (+SDS) were loaded as a positive control. WT substrate prepared from Sf9 cells in the presence of SDS (+SDS) appeared at approximately 15 kDa, as seen in SDS-PAGE, indicating the monomeric band as a positive control. However, monomeric band of lysates in transfected cells from WT in the presence of SDS (+SDS) failed to be detected. WT substrate prepared from Sf9 cells in the absence of SDS (−SDS) was loaded as indicators of monomer, dimer, and trimer. (B) is low-contrast version of (A).

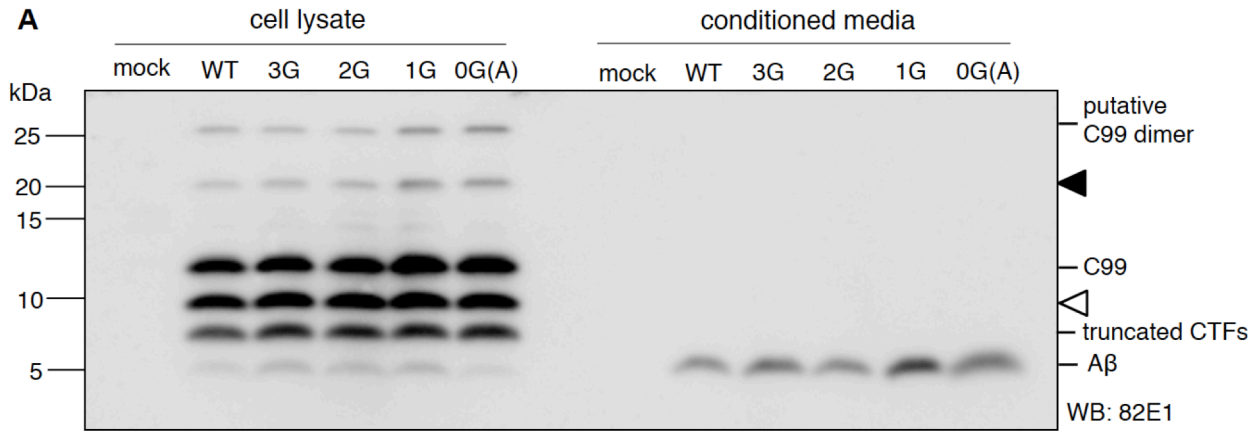
A
cell lysate
conditioned media
mock
WT
3G
2G
1G
0G(A)
mock
WT
3G
2G
1G
0G(A)
kDa
25
20
15
10
5
putative
C99 dimer
C99
truncated CTFs
Aβ
WB: 82E1

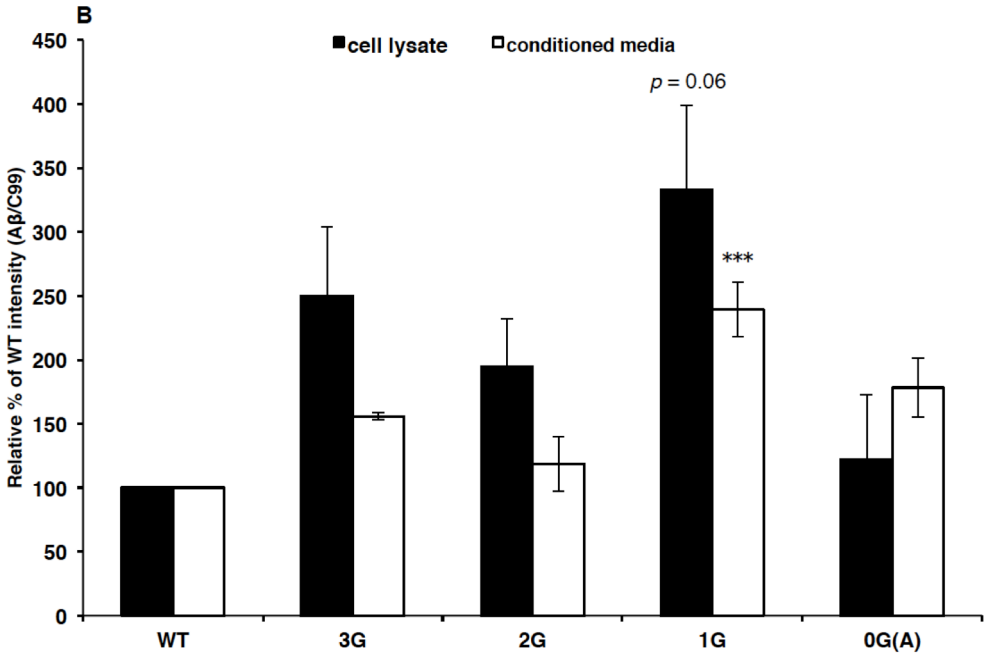
B
cell lysate
conditioned media
p = 0.06
***
Relative % of WT intensity (Aβ/C99)
450
400
350
300
250
200
150
100
50
0
WT
3G
2G
1G
0G(A)

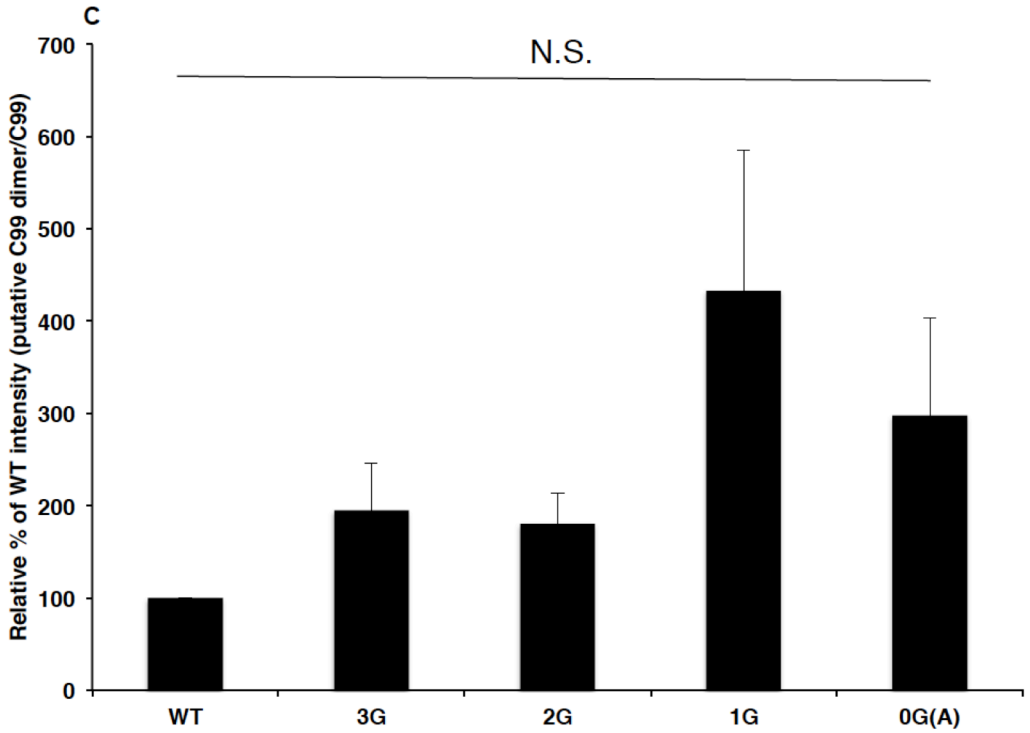
C
N.S.
Relative % of WT intensity (putative C99 dimer/C99)
700
600
500
400
300
200
100
0
WT
3G
2G
1G
0G(A)

Figure 3-2. Effects of alanine substitution on Aβ production from each mutant. (A) Conditioned media and cell lysate from each mutant were subjected to Western blotting with 82E1 antibody to detect Aβ. Open and closed arrowheads in (A) indicate a potential caspase-cleaved product and its putative dimer, respectively (Gervais *et al*. 1999). (B) The band intensities of Aβ in the cell lysate, conditioned media, and C99 were measured using a LAS-4000 luminescent image analyzer. The ratio of Aβ/C99 was calculated. Band intensity of Aβ/C99 in wild type (WT) was set at 100%. Aβ production in conditioned media from 1G was significantly increased compared with that in WT (white bar), and Aβ production in the cell lysate tended to increase for all mutants (black bar). (C) The band intensities of putative C99 dimer and C99 were measured using a LAS-4000 luminescent image analyzer. The ratio of putative C99 dimer/C99 was calculated. Band intensity of putative C99 dimer/C99 in WT was set at 100%. No significant differences were observed between any mutant and WT in the ratio of putative C99 dimer/C99. Data are expressed as mean ± SEM (n = 3, ***: $p < 0.005$, ANOVA with Holm−Sidak's post hoc test compared with WT).

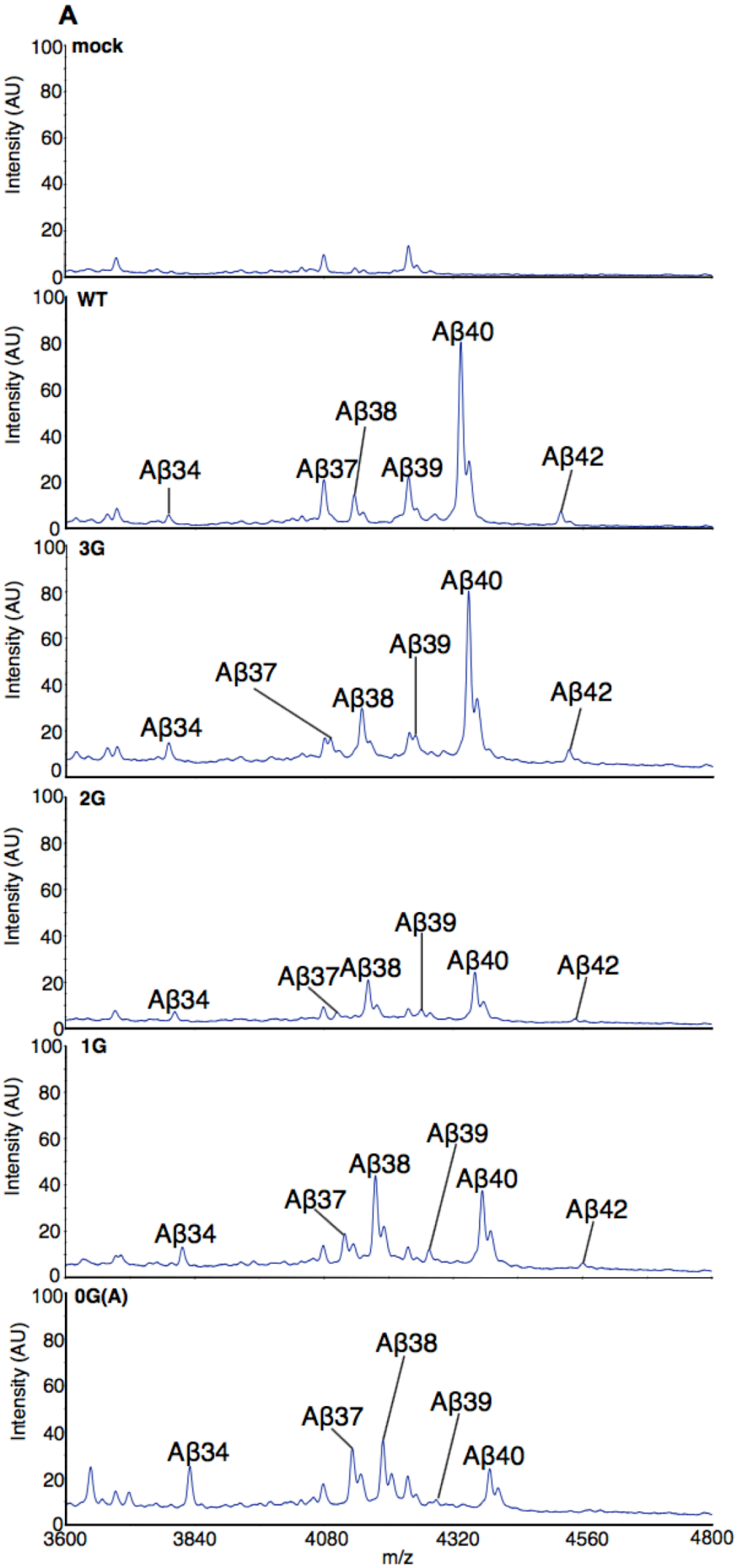
A
mock
WT
3G
2G
1G
0G(A)
Intensity (AU)
Aβ34
Aβ37
Aβ38
Aβ39
Aβ40
Aβ42
m/z
3600
3840
4080
4320
4560
4800

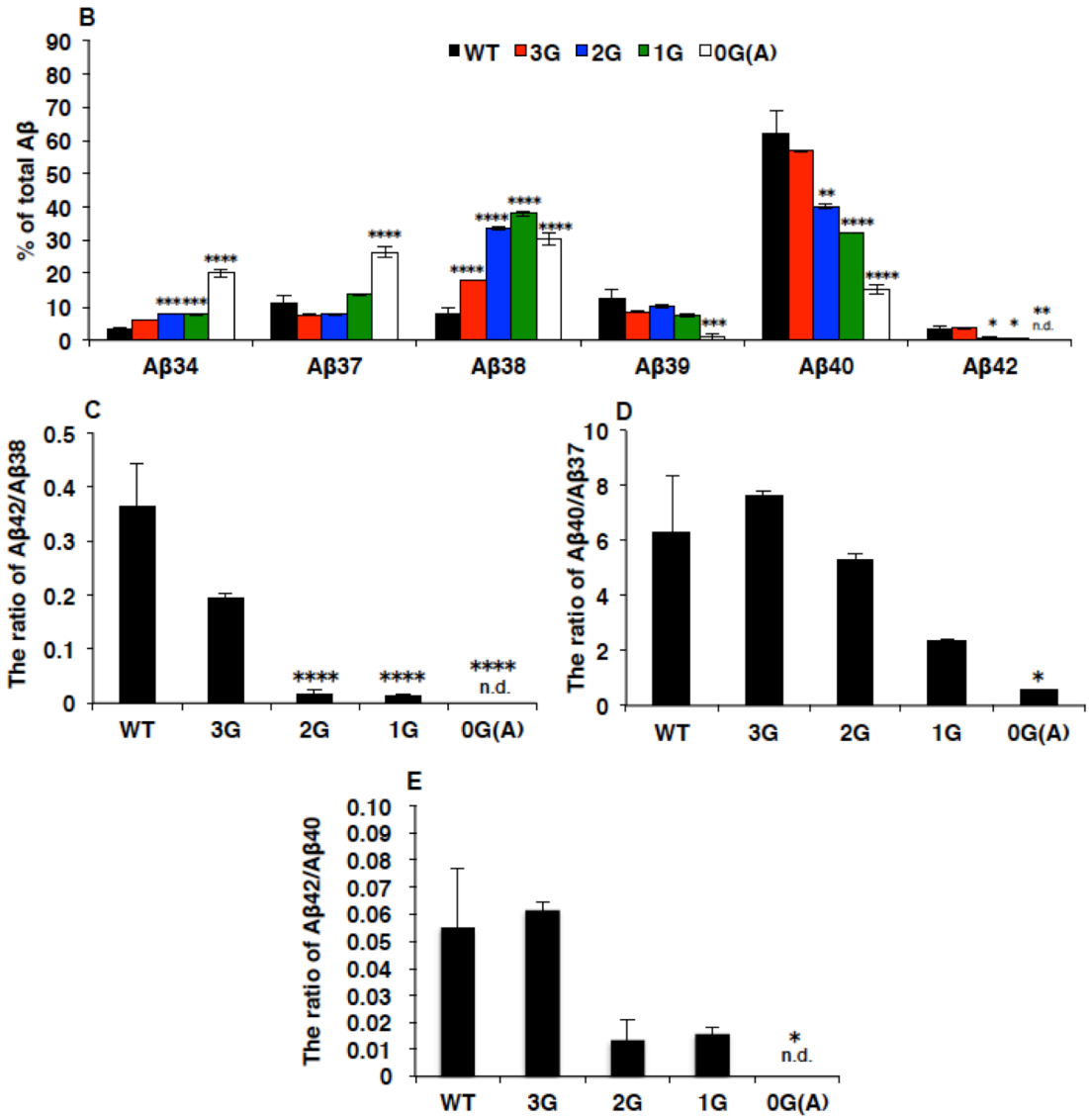

Figure 3-3. Production of Aβ species modulated by alanine substitution in conditioned media from each mutant. (A) Production of Aβ species modulated by alanine substitution. Total Aβ produced from conditioned media from each mutant was immunoprecipitated with 4G8 antibody and subjected to matrix-assisted laser desorption/ionization time-of-flight mass spectrometry (MALDI-TOF-MS). (B) Percentage of Aβ species from each C99-FLAG substrate was calculated by MS using peak intensity. The sum of all peak intensities was set as 100%, and the percentage of each Aβ species was calculated. Percentages of Aβ40 and Aβ42 decreased for 2G, 1G, and 0G (A), and the ratio of Aβ38 increased in all mutants. In addition, the production of short Aβ species (e.g., Aβ34) was elevated for 2G, 1G, and 0G (A). (C and D) Ratios of Aβ40/Aβ37 and Aβ42/Aβ38, which indicate the ratios of precursor/product, respectively. These ratios tended to decrease for all mutants. (E) Ratio of Aβ42/Aβ40. I calculated the ratio using the percentage of each Aβ species calculated in (B). The ratio tended to decrease for all mutants. Data are expressed as mean ± SEM (n = 3, *: $p < 0.05$; **: $p < 0.01$; ***: $p < 0.005$; ****: $p < 0.001$, ANOVA with Holm−Sidak's post hoc test compared with WT). n.d. indicates not detected.

General Discussion

In this thesis study, I showed the following findings. (1) Substitutions in the GXXXG motifs failed to alter C99 dimerization in an *in vitro* assay using detergent-solubilized substrate and BN-PAGE. (2) Cell-based and solubilized γ-secretase assays demonstrated that substitutions in the motifs decreased the production of long Aβ species such as Aβ42 and Aβ43 and increased short Aβ species such as Aβ34. (3) Both assays demonstrated that substitutions in the motifs decreased the ratios of precursor/product and Aβ42/Aβ40.

The transmembrane domain of C99 is thought to take the canonical α-helical structure (Lichtenthaler *et al.* 1999b). Based on this assumption, the hypothetical model of γ-secretase processing has been proposed: successive removal of three or four amino acid residues from either Aβ48 or Aβ49 (Takami *et al.* 2009; Matsumura *et al.* 2014; Takami and Funamoto 2012; Yagishita *et al.* 2008). Because the canonical α-helix takes a single turn with 3.6 residues on average, amino acid residues appear every three or four residues on a face of the helix. For example, the carboxyl sides of the 37th residue and the 34th residue are aligned on the same face of the α-helical surface with that of the 40th residue offset slightly (Fig. 4A). As such, it is reasonable to consider that Aβ34 is produced from the Aβ40 production pathway. In detail, Aβ40 would be successively cleaved into Aβ34 via Aβ37 (Aβ40 > Aβ37 > Aβ34), releasing tripeptide (Fig. 4B). If γ-secretase cleaves the peptide bond on or around one face of the helix, it would cleave off three or four residues at a time. In fact, the previous studies succeeded in detecting tri- or tetra-peptide generated successively from

longer Aβ species (Takami *et al.* 2009; Matsumura *et al.* 2014; Takami and Funamoto 2012; Yagishita *et al.* 2008).

Transmembrane domain length varies extensively from 15 to 40 amino acid residues (Bowie 1997). Given that the thickness of the biological membrane is around 3~5 nm (Watson 2015), this large variability in length suggests that a transmembrane domain takes multiple secondary structures other than the canonical α-helix, which has a 0.15 nm rise/residue (1.5 Å). In fact, it is common that transmembrane helices contain some other structures such as 3_{10}-helices, wide turns, and kinks. Although structural mechanisms of how they occur remains largely unknown, several studies have looked at what amino acid tend to be more associated to these structures. Particularly, the propensity of each amino acid to generate a bend has been extensively studied in model proteins and verified against known protein structures (Monné *et al.* 1999). In this classification, Gly is the second most residues, following Pro, to induce a bend. Interestingly, Ala, Leu, and Phe, which I used to replace Gly in the GXXXG motifs, are the least three residues to make a turn in a helix. Based on these findings, I speculate that the substitutions of Gly to Ala, Leu, or Phe in the GXXXG motifs change the helical wrapping of the transmembrane domain, thereby facilitating the successive processing of Aβ42 and Aβ43 toward the amino-terminal end to generate shorter Aβ species (see Figs. 2-7 and 2-8). In addition, Gly is a polar amino acid, whereas Ala, Leu, and Phe are hydrophobic amino acids. Based on the propensity, mutations decrease the ratio of

polar amino acids and increase that of hydrophobic amino acids within the transmembrane domain (Fig. 5). This might support the speculation that substitutions in the GXXXG motifs change the helical wrapping of the transmembrane domain.

These might be a part of the reason why the production of Aβ42 and Aβ43 increases in AD. Two of the GXXXG motifs of C99 are predicted to be in the lipid bilayer. They have been implicated not only in the dimerization but also in the intramembrane interaction with cholesterol (Barrett *et al.* 2012). The lipid environment in the membrane might affect the structure of transmembrane helix. For example, most of membrane proteins expressed on surface must initially adapt to the thinner lipid bilayer of the ER, which causes the hydrophobic mismatch, by adjusting the surrounding lipids and/or the transmembrane structure. Therefore, alterations in the lipid composition around the transmembrane GXXXG motifs may also affect the helical structure of C99 in a similar manner to the amino acid substitutions. In AD, there is a line of evidence that the lipid composition in the membrane is altered (Pettegrew *et al.* 2001). Also, it has been reported that the lipid environment affects γ-processing (Wolozin 2004; Grimm *et al.* 2007; Piao *et al.* 2013).

Jung and colleagues, using a mutation involving the GXXXG motif (G29K/A30K), reported that γ-secretase preferentially cleaved monomeric C99 rather than its dimer (Jung *et al.* 2014). In contrast, my data indicated that, although the ratios of monomer to dimer for the mutants showed a similar trend to that observed by Jung *et al.*, the cleavage efficiency of γ-secretase differed (see Figs

2-2 and 2-6). These findings suggest that the cleavage efficiency might not always correlate with the tendency to form monomeric C99. Although the stoichiometry of the binding between γ-secretase and substrate remains unknown, it is reasonable to propose a one-to-one relationship between γ-secretase and substrate during the reaction.

In conclusion, my thesis study identified a novel role of the GXXXG motif in C99 on γ-processing and Aβ production. My findings might be useful for a development of new ways of therapeutic interventions. Because the amino acid substitutions in the GXXXG motifs reduced the levels of amyloidogenic Aβ production, drugs targeted to the GXXXG motifs would reduce Aβ42 and Aβ43, thereby inhibiting the formation of amyloid plaques.

Figures

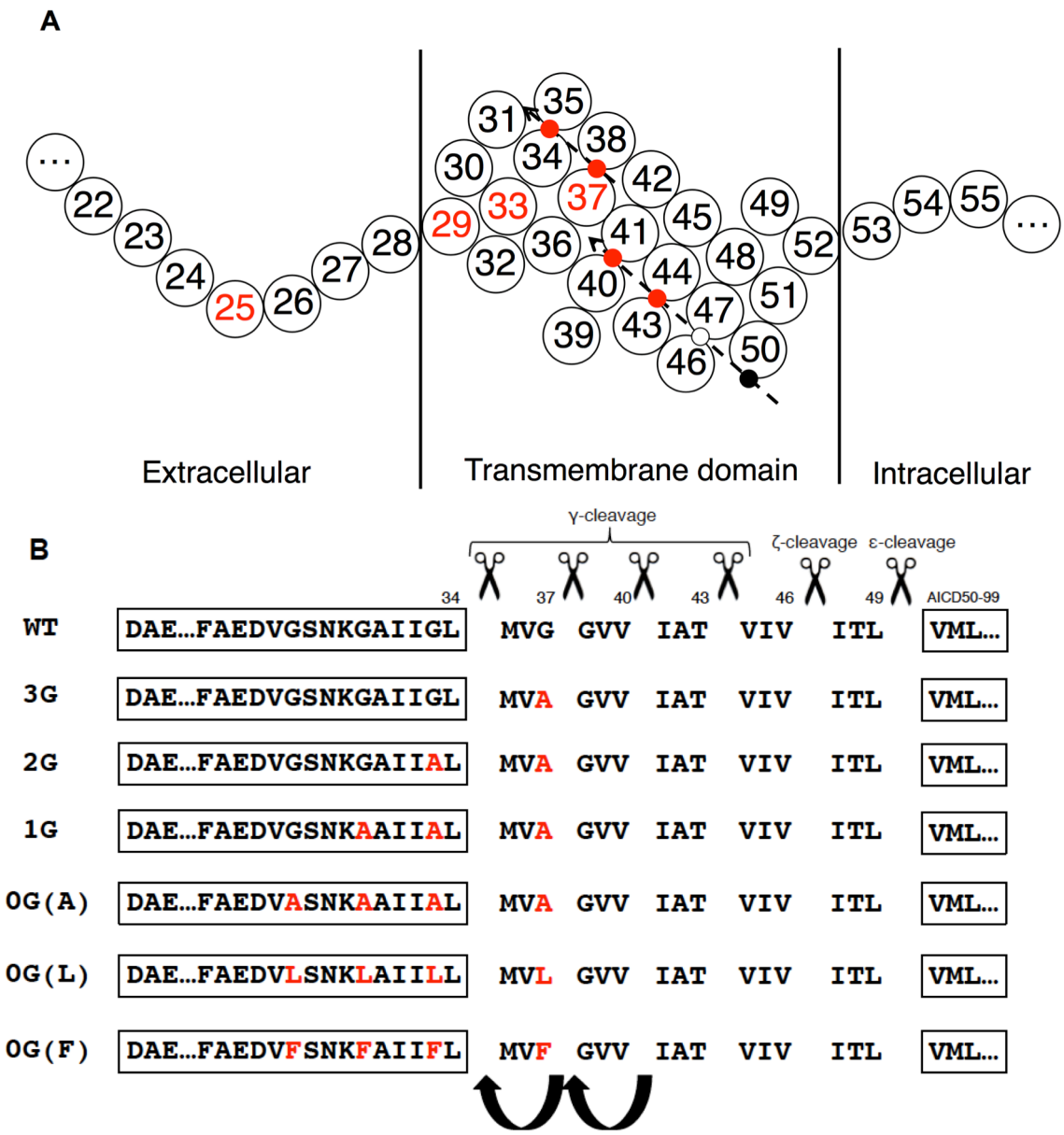

Figure 4. Schematic representation of putative Aβ34 product line. (A) A side view of the α-helix of the transmembrane domain of APP. The number represents Aβ numbering. The red number indicates the G of the GXXXG motifs. The carboxyl sides of the 37th residue and the 34th residue are aligned on the same side of the α-helical surface. Black circle, white circle and red circle represent ε-cleavage, ζ-cleavage, and γ-cleavage, respectively. (B) γ-Secretase cleaves C99 in stepwise manner in a direction from the ε-cleavage (right scissors) to γ-cleavage sites (left scissors) of Aβ49 by releasing tripeptides at every helical turn or plus an additional tertapeptide, finally producing Aβ40 (Takami *et al.* 2009). From this perspective, γ-secretase would cleave further from Aβ40; consequently, Aβ34 would successively produce cleavage from Aβ40 via Aβ37. These figures are modified from the papers by Qi-Takahara *et al.* (2005) and Takami *et al.* (2009).

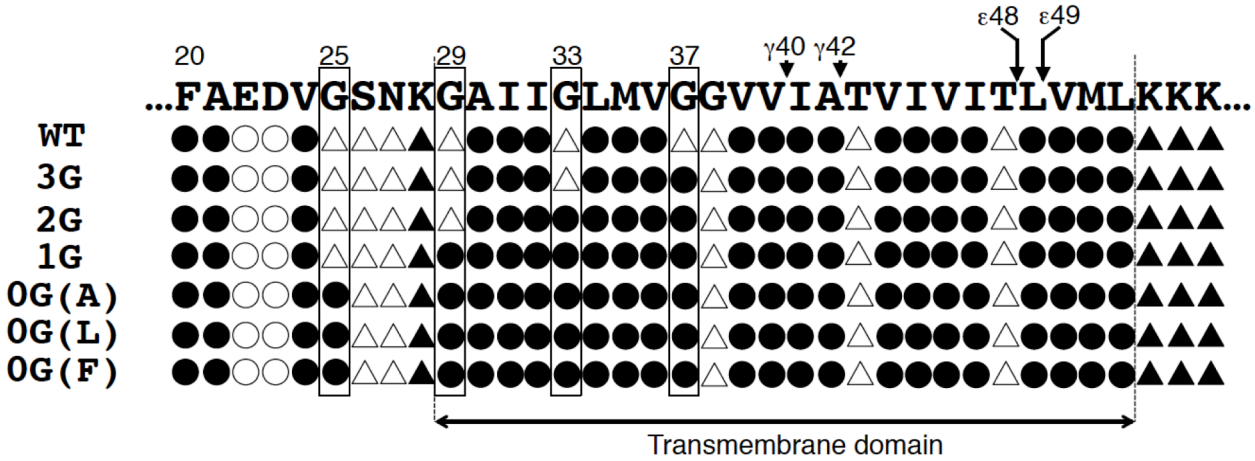

Figure 5. Sequence classification of C99. The sequence of C99 is classified, in accordance with properties of amino acids. The number represents Aβ numbering. Rectangles, arrowheads and arrows represent the G of the GXXXG motifs, γ-cleavage site, and ε-cleavage site, respectively. Black circles, white circles, black triangles, and white triangles represent hydrophobic amino acids, acidic amino acids, basic amino acids, and polar amino acids, respectively. From these perspectives, mutations decrease the ratio of polar amino acids and increase that of hydrophobic amino acids within the transmembrane domain.

Acknowledgments

First, I would like to express my sincere gratitude my advisors, Dr. Yasuo Ihara and Dr. Nobuyuki Nukina for their support, invaluable guidance and teachings, and all the aid I received from then during the development of this research and writing of this document. I also extend my feelings of gratitude to my thesis reviewing committee: Dr. Hiroaki Misonou, Dr. Shigeo Takamori, and Dr. Fumino Fujiyama, for the useful discussions. Advice and comments given by them has been a great help in widening my research from various perspectives.

I would like to thank to Dr. Shigeichi Shono (Doshisha University, Kyoto, Japan) for mass spectrometry operation, to Ms. Seiko Ishihara and Ms. Mika Nobuhara (Doshisha University, Kyoto, Japan) for technical supports and preparing substrates of 0G (L) and 0G (F), to Ms. Asuka Kokawa (Tokyo University, Tokyo, Japan) for preparing substrates of WT, to Dr. Taisuke Tomita and Dr. Takeshi Iwatsubo (Tokyo University, Tokyo, Japan) for anti-presenilin 1-CTF antiserum, and to Dr. Nobuto Kakuda, Dr. Tomohiro Miyasaka, and Dr. Satoru Funamoto for giving insightful comments and suggestions of this research.

This work was supported in part by the MEXT-Supported Program for the Strategic Research Foundation at Private Universities (to Dr. Yasuo Ihara).

Abbreviation List

2D: two-dimensional.

Aβ: Amyloid β.

AD: Alzheimer's disease.

AICD: APP intracellular domain.

ANOVA: analysis of variance.

Aph-1: anterior pharynx defective-1.

APP: Amyloid precursor protein.

BN-PAGE: blue native polyacrylamide gel electrophoresis.

BSA: bovine serum albumin.

C99: carboxyl terminal fragment of APP.

CBB: Coomassie Brilliant Blue.

CHAPS: 3-[(3-cholamidopropyl)dimethylammonio]-1-propanesulfonate.

CHAPSO: 3-[(3-cholamidopropyl)dimethylammonio]-2-hydroxyl-1-propanesulfonate.

CHCA: α-cyano-4-hydroxycinnamic acid.

CHO: Chinese Hamster Ovary.

CSF: cerebrospinal fluid.

CTF: carboxyl terminal fragment.

DAPT: N-[N-(3,5-difluorophenacetyl)-L-alanyl]-S-phenylglycine t-butyl ester.

DDM: n-dodecyl-β-D-maltoside.

DMA: N, N-dimethylacetamide.

EGTA: ethylene glycol tetraacetic acid.

ER: endoplasmic reticulum.

FBS: fetal bovine serum.

kDa: kilo dalton.

MALDI-TOF-MS: matrix-assisted laser desorption/ionization time of flight mass spectrometry.

MCI: mild cognitive impairment.

MEF: mouse embryonic fibroblast.

Nct: nicastrin.

n.d.: not detected.

NFT: neurofibrillary tangles.

N.S.: not significant.

PAGE: polyacrylamide gel electrophoresis.

PBS: phosphate-buffered saline.

PCR: polymerase chain reaction.

Pen-2: presenilin enhancer-2.

PIPES: piperazine-N, N′-bis (2-ethanesulfonic acid).

PS1: presenilin 1.

PVDF: polyvinylidene difluoride.

SDS: sodium dodecyl sulfate.

SEM: standard error of the mean.

TBS: Tris-buffered saline.

TLCK: 1-chloro-3-tosylamido-7-amino-2-heptanone.

Tricine: N-[2-hydroxy-1,1-bis(hydroxymethyl)ethyl]glycine.

Triton X-100: polyethylene glycol mono-*p*-isooctyl phenyl ether.

WT: wild type.

References

1. Araki W., Saito S., Takahashi-Sasaki N., Shiraishi H., Komano H., and Murayama K. S. (2006) Characterization of APH-1 mutants with a disrupted transmembrane GxxxG motif. *J. Mol. Neurosci.* **29,** 35–43.

2. Asami-Odaka A., Ishibashi Y., Kikuchi T., Kitada C., and Suziki N. (1995) Long Amyloid β-protein Secreted from Wild-Type Human Neuroblastoma IMR-32 Cells. *Biochem.* **34,** 10272-10278.

3. Baulac S., LaVoie M.J., Kimberly W.T., Strahle J., Wolfe M.S., Selkoe D.J., and Xia W. (2003). Functional γ-secretase complex assembly in Golgi/trans-Golgi network: interactions among presenilin, nicastrin, Aph1, Pen-2, and γ-secretase substrates. *Neurobiology of Disease*. **14,** 194–204.

4. Barrett P.J., Song Y., Van Horn W.D., Hustedt E.J., Schafer J.M., Hadziselimovic A., Beel A.J., and Sanders C.R. (2012) The Amyloid precursor protein has a flexible transmembrane domain and binds cholesterol. *Science.* **336,** 1168-1171.

5. Bowie J.U. (1997) Helix packing in membrane proteins. *J Mol Bio.* **272,** 780-789.

6. Burns A. and Iliffe S. (2009) Alzheimer's disease. *BMJ*. **338**, 467-471.

7. Capell A., Beher D., Prokop S., Steiner H., Kaether C., Shearman M.S., and Haass C. (2005). γ-Secretase Complex Assembly within the Early Secretory Pathway. *J. Biol. Chem*. **280,** 6471–6478.

8. Chávez-Gutiérrez L., Bammens L., Benilova I., Vandersteen A., Benurwar M., Borgers M., Lismont S., Zhou L., Van Cleynenbreugel S., Esselmann H., Wiltfang J., Serneels L., Karran E., Gijsen H., Schymkowitz J., Rousseau F., Broersen K., and De Strooper B. (2012) The mechanism of γ-Secretase dysfunction in familial Alzheimer disease. *EMBO J.* **31,** 2261-2274.

9. Cladera J., Ricaud, J.L.,Villaverde J., and DuNach M. (1997). Liposome Solubilization and Membrane Protein Reconstitution Using Chaps and Chapso. *European Journal of Biochemistry*. **243**, 798–804.

10. De Jonghe C., Esselens C., Kumar-Singh S., Craessaerts K., Serneels S., Checler F., Annaert W., Van Broeckhoven C., and De Strooper B. (2001) Pathogenic APP mutations near the γ-secretase cleavage site differentially affect Aβ secretion and APP C-terminal fragment stability. *Hum Mol Genet,* **10,** 1665-1671.

11. Decock M., Stanga S., Octave J.N., Dewachter I., Smith S. O., Constantinescu S.N., and Kienlen-Campard P. (2016) Glycines from the APP GXXXG/GXXXA Transmembrane Motifs Promote Formation of Pathogenic Aβ Oligomers in Cells. *Front Aging Neurosci.* **107,** doi: 10.3389/fnagi.2016.00107.

12. De Strooper B., Annaert W., Cupers P., Saftig P., Craessaerts K., Mumm J.S., Schroeter E.H., Schrijvers V., Wolfe M.S., Ray W.J., Goate A., and Kopan R. (1999). A presenilin-1-dependent γ-secretase-like protease mediates release of Notch intracellular domain. *Nature*. **398**, 518–522.

13. Dovey H.F., John V., Anderson J.P., Chen L.Z., de Saint Andrieu P, Fang L.Y., Freedman S.B., Folmer B., Goldbach E., Holsztynska E.J., Hu K.L., Johnson-Wood K.L., Kennedy S.L., Kholodenko D., Knops J.E., Latimer L.H., Lee M., Liao Z., Lieberburg I.M., Motter R.N., Mutter L.C., Nietz J., Quinn K.P., Sacchi K.L., Seubert P.A., Shopp G.M., Thorsett E.D., Tung J.S., Wu J., Yang S., Yin C.T., Schenk D.B., May P.C., Altstiel L.D., Bender M.H., Boggs L.N., Britton T.C., Clemens J.C., Czilli D.L., Dieckman-McGinty D.K., Droste J.J., Fuson K.S., Gitter B.D., Hyslop P.A., Johnstone E.M., Li W.Y., Little SP, Mabry T.E., Miller F.D., and Audia J.E. (2001) Functional gamma-secretase inhibitors reduce beta-amyloid peptide levels in brain. *J. Neurochem.* **76,** 173-181.

14. Fraering P.C., Ye W., Strub J.M., Dolios G., LaVoie M.J., Ostaszewski B.L., van Dorsselaer A., Wang R., Selkoe D.J., and Wolfe M.S. (2004) Purification and characterization of the human γ-secretase complex. *Biochemistry.* **43,** 9774-9789.

15. Francis R., McGrath G., Zhang J., Ruddy D.A., Sym M., Apfeld J., Nicoll M., Maxwell M., Hai B., Ellis M.C., Parks A.L., Xu W., Li J., Gurney M., Myers R.L., Himes C.S., Hiebsch R., Ruble C., Nye J.S., and Curtis D. (2002). aph-1 and pen-2 are required for Notch pathway signaling, γ-secretase cleavage of βAPP, and presenilin protein accumulation. *Dev Cell* **3,** 85-97.

16. Funamoto S., Morishima-Kawashima M., Tanimura Y., Hirotani N., Saido T.C., and Ihara Y. (2004) Truncated carboxyl-terminal fragments of β-amyloid precursor protein are processed to amyloid β-proteins 40 and 42. *Biochemistry.* **43,** 13532-13540.

17. Funamoto S., Sasaki T., Ishihara S., Nobuhara M., Nakano M., Watanabe-Takahashi M., Saito T., Kakuda N., Miyasaka T., Nishikawa K., Saido T.C., and Ihara Y. (2013) Substrate ectodomain is critical for substrate preference and inhibition of γ-secretase. *Nature Commun* **2529,** doi: 10.1038/ncomms3529.

18. Furthmayr H. and Marchesi V.T. (1976) Subunit structure of human erythrocyte glycophorin A. *Biochemistry.* **15,** 1137-1144.

19. Gervais F. G., Xu D., Robertson G. S., Vaillancourt J. P., ZhuY., Huang J., LeBlanc A., Smith D., Rigby M., Shearman M.S., Clarke E. E., Zheng H., Van Der Ploeg L. H., Ruffolo S. C., Thornberry N. A., Xanthoudakis S., Zamboni R. J., Roy S., and Nicholson D. W. (1999) Involvement of Caspases in Proteolytic Cleavage of Alzheimer's Amyloid-β Precursor Protein and Amyloidogenic Aβ Peptide Formation, *Cell* **97,** 395-406.

20. Glenner G.G. and Wong C.W. (1984a) Alzheimer's disease: initial report of the purification and characterization of a novel cerebrovascular amyloid protein. *Biochem Biophys Res Commun.* **120,** 885-890.

21. Glenner G.G. and Wong C.W. (1984b) Alzheimer's disease and Down's syndrome: sharing of a unique cerebrovascular amyloid fibril protein. *Biochem Biophys Res Commun.* **122,** 1131-1135.

22. Goutte C., Tsunozaki M., Hale V.A., and Priess J.R. (2002). APH-1 is a multipass membrane protein essential for the Notch signaling pathway in Caenorhabditis elegans embryos. *Proc Natl Acad Sci USA* **99,** 775-779.

23. Grimm M.O., Grimm H.S., and Hartmann T. (2007) Amyloid beta as a regulator of lipid homeostasis. *Trends Mol Med.* **13,** 337-344.

24. Gu Y., Chen F., Sanjo N., Kawarai T., Hasegawa H., Duthie M., Li W., Ruan X., Luthra A., Mount H. T., Tandon A., Fraser P. E., and St George-Hyslop P. (2003) APH-1 Interacts with Mature and Immature Forms of Presenilins and Nicastrin and May Play a Role in Maturation of Presenilin·Nicastrin Complexes. *J. Biol. Chem.* **278,** 7374–7380.

25. Gu Y., Misonou H., Sato T., Dohmae N., Takio K., and Ihara Y. (2001) Distinct intramembrane cleavage of the β-amyloid precursor protein family resembling γ-secretase-like cleavage of Notch. *J. Biol. Chem.* **276,** 35235-35238.

26. Haass C., Hung A.Y., and Selkoe D.J. (1991) Processing of β-amyloid precursor protein in microglia and astrocytes favors an internal localization over constitutive secretion. *J NeuroSci.* **11,** 3783-3893.

27. Haass C., Schlossmacher M.G., Hung A.Y., Vigo-Pelfrey C., Mellon A., Ostaszewski B.L., Lieberburg I., Koo E., Schenk D., Teplow D.B., and Selkoe D.J. (1992) Amyloid β-peptide is produced by cultured cells during normal metabolism. *Nature.* **357,** 500-503.

28. Haffner C., Frauli M., Topp S., Irmler M., Hofmann K., Regula J.T., Bally-Cuif L., Haass C. (2004). Nicalin and its binding partner Nomo are novel Nodal signaling antagonists *EMBO J.* **23,** 3041–3050.

29. Hardy J.A. and Higgins G.A. (1992) Alzheimer's disease: the amyloid cascade hypothesis. *Science* **256**, 184-185.

30. Hayashi I., Urano Y., Fukuda R., Isoo N., Kodama T., Hamakubo T., Tomita T., and Iwatsubo T. (2004) Selective Reconstitution and Recovery of Functional γ-Secretase Complex on Budded Baculovirus Particles. *J. Biol. Chem.* **279,** 38040-38046.

31. Hu Y. and Fortini M. E. (2003) Different cofactor activities in γ-secretase assembly: evidence for a nicastrin-Aph-1 subcomplex. *J. Cell Biol.* **161,** 685–690.

32. Ida N., Hartmann T., Pantel J., Schröder J., Zerfass R., Förstl H., Sandbrink R., Masters C.L., and Beyreuther K. (1996) Analysis of heterogeneous A4 peptides in human cerebrospinal fluid and blood by a newly developed sensitive Western blot assay. *J. Biol. Chem.* **271,** 22908-22914.

33. Iwatsubo T. Odaka A., Suzuki N., Mizusawa H., Nukina N., and Ihara Y. (1994) Visualization of Aβ42(43) and Aβ40 in senile plaques with end-specific Aβ monoclonals: Evidence that an initially deposited species is Aβ42(43). *Neuron.* **13,** 45-53.

34. Jung J.I., Premraj S., Cruz P.E., Ladd T.B., Kwak Y., Koo E.H., Felsenstein K.M., Golde T.E., and Ran Y. (2014) Independent Relationship between Amyloid Precursor Protein (APP) Dimerization and γ-Secretase Processivity. *PLOS ONE* **9,** e111553.

35. Kaether C, Haass C., and Steiner H. (2006) Assembly, trafficking and function of γ-secretase. *Neurodegener Dis.* **3**, 275-283.

36. Kakuda N., Akazawa K., Hatsuta H., Murayama S., and Ihara Y. (2013) Suspected limited efficacy of γ-secretase modulators. *Neurobiol. Aging.* **34,** 1101-1104.

37. Kakuda N., Funamoto S., Yagishita S., Takami M. Osawa S, Dohmae E., and Ihara Y. (2006) Equimolar Production of Amyloid β-Protein and Amyloid Precursor Protein Intracellular Domain from β-Carboxyl-terminal Fragment by γ-Secretase. *J. Biol. Chem.* **281**, 14776-14786.

38. Kakuda N., Shoji M., Arai H., Furukawa K., Ikeuchi T., Akazawa K., Takami M., Hatsuta H., Murayama S., Hashimoto Y., Miyajima M., Arai H., Nagashima Y., Yamaguchi H., Kuwano R., Nagaike K., and Ihara Y. (2012) Altered γ-secretase activity in mild cognitive impairment and Alzheimer's disease. *EMBO Mol. Med.* **4**, 344-352.

39. Kang J., Lemaire H.G., Unterbeck A., Salbaum J.M., Masters C.L., Grzeschik K.H., Multhaup G., Beyreuther K., and Müller-Hill B. (1987) The precursor of Alzheimer's disease amyloid A4 protein resembles a cell-surface receptor. *Nature.* **325,** 733-736.

40. Kienlen-Campard P., Tasiaux B., Van Hees J., Li M., Huysseune S., Sato T., Fei J.Z., Aimoto S., Courtoy P.J., Smith S.O., Constantinescu S.N., and Octave J.N. (2008) Amyloidgenic Processing but Not Amyloid Precursor Protein (APP) Intracellular C-terminal Domain Production Requires a Precisely Oriented APP Dimer Assembles by Transmembrane GXXXG Motifs. *J. Biol. Chem*. **283**, 7733-7744.

41. Kim S.H., Ikeuchi T., Yu C.J., and Sisodia S.S. (2003) Regulated Hyperaccumulation of Presenilin-1 and the "γ-secretase" complex. EVIDENCE FOR DIFFERENTIAL INTRAMEMBRANOUS PROCESSING OF TRANSMEMBRANE SUBSTRATES. *J. Biol. Chem.* **278,** 33992–34002.

42. Kim S.H., Yin Y.I., Li Y.M., and Sisodia S.S. (2004). Evidence That Assembly of an Active γ-Secretase Complex Occurs in the Early Compartments of the Secretory Pathway. *J. Biol. Chem*. **279**, 48615–48619.

43. Kokawa A., Ishihara S., Fujiwara H., Nobuhara M., Iwata M., Ihara Y., and Funamoto S. (2015) The A673T mutation in the amyloid precursor protein reduces the production of β-amyloid protein from its β-carboxyl terminal fragment in cells. *Acta Neuropathol Commun.* **3:66,** DOI: 10.1186/s40478-015-0247-6.

44. Koo E.H., Park L., and Selkoe D.J. (1993) Amyloid β-protein as a substrate interacts with extracellular matrix to promote neurite outgrowth. *Proc Natl Acad Sci*. **90,** 4748-4752.

45. Kumar D.K., Choi S.H., Washicosky K.J., Eimer W.A., Tucker S., Ghofrani J., Lefkowitz A., McColl G., Goldstein L.E., Tanzi R.E., and Moir R.D. (2016) Amyloid-β peptides protects against microbial infection in mouse and worm models of Alzheimer's disease. *Sci Transl Med.* **8,** 340ra372.

46. Laudon H., Hansson E.M., Melén K., Bergman A., Farmery M.R., Winblad B., Lendahl U., von Heijne G., and Näslund J. (2005). A nine-transmembrane domain topology for presenilin 1. *J. Biol. Chem*. **280**, 35352–35360.

47. LaVoie M.J., Fraering P.C., Ostaszewski B.L., Ye W.J., Kimberly W.T., Wolfe M.S., and Selkoe D.J. (2003) Assembly of the γ-Secretase Complex Involves Early Formation of an Intermediate Subcomplex of Aph-1 and Nicastrin. *J. Biol. Chem.* **278,** 37213–37222.

48. Lee S.F., Shah S., Yu C., Wigley W.C., Li H., Lim M., Pedersen K., Han W., Thomas P., Lundkvist J., Hao Y.H., and Yu G. (2004) A Conserved GXXXG Motif in APH-1 Is Critical for Assembly and Activity of the γ-Secretase Complex. *J. Biol. Chem.* **279**, 4144-4152.

49. Li Y. M., Lai M. T., Xu M., Huang Q., DiMuzio-Mower J., Sardana M. K., Shi X. P., Yin K. C., Shafer J. A., and Gardell S. J. (2000) Presenilin 1 is linked with γ-secretase activity in the detergent solubilized state. *Proc. Natl. Acad. Sci.* U. S. A. **97,** 6138–6143.

50. Lichtenthaler S.F., Multhaup G., Masters C.L., and Beyreuther K. (1999a) A novel substrate for analyzing Alzheimer's disease γ-secretase. *FEBS Lett.* **453,** 288-292.

51. Lichtenthaler S.F., Wang R., Grimm H., Uljon S.N., Masters C.L., Beyreuther K. (1999b) Mechanism of the cleavage specificity of Alzheimer's disease γ-secretase identified by phenylalanine-scanning mutagenesis of the transmembrane domain of the amyloid precursor protein. *Proc Natl Acad Sci*. **96,** 3053-3058.

52. Lu P., Bai X.C., Ma D. Xie T., Yan C., Sun L., Yang G., Zhao Y., Zhou R., Scheres S.H. and Shi Y. (2014) Three-dimensional structure of human γ-secretase. *Nature.* **512,** 166-170.

53. Luo W. J., Wang H., Li H., Kim B.S., Shah S., Lee H.J., Thinakaran G., Kim T. W., Yu G., and Xu H. (2003) PEN-2 and APH-1 Coordinately Regulate Proteolytic Processing of Presenilin 1. *J. Biol. Chem.* **278,** 7850–7854.

54. Marambaud P., Shioi J., Serban G., Georgakopoulos A., Sarner S., Nagy V., Baki L., Wen P., Efthimiopoulos S., Shao Z., Wisniewski T., and Robakis N.K. (2002). A presenilin-1/γ-secretase cleavage releases the E-cadherin intracellular domain and regulates disassembly of adherens junctions. *EMBO J.* **21,** 1948–1956.

55. Marinangeli C., Tasiaux B., Opsomer R., Hage S., Sodero A.O., Dewachter I., Octave J.N, Smith S.O., Constantinescu S.N., and Kienlen-Campard P. (2015) Presenilin transmembrane domain 8 conserved AXXXAXXXG motifs are required for the activity of the γ-secretase complex. *J. Biol. Chem.* **290**, 7169-7184.

56. Martin B.L., Schrader-Fischer G., Busciglio J., Duke M., Paganetti P., and Yankner B.A. (1995) Intracellular accumulation of β-amyloid in cells expressing the Swedish mutant amyloid precursor protein. *J Biol. Chem.* **270,** 26727-26730.

57. Masters C.L., Simms G, Weinman N.A., Multhaup G., McDonald B.L., and Beyreuther K. (1985a) Amyloid plaque core protein in Alzheimer's disease and Down syndrome. *Proc. Natl. Acad. Sci. U.S.A*. **82**, 4245-4249.

58. Masters C.L., Multhaup G., Simms G., Pottgiesser J., Martins R.N., and Beyreuther K. (1985b) Neuronal origin of a cerebral amyloid: neurofibrillary tangles of Alzheimer's disease contain the same protein as the amyloid of plaque cores and blood vessels. *EMBO J.* **4,** 2757-2763.

59. Matsumura N., Takami M., Okochi M., Wada-Kakuda S., Fujiwara H., Tagami S., Funamoto S., Ihara Y., and Morishima-Kawashima M. (2014) γ-Secretase associated with lipid rafts: multiple interactive pathways in the stepwise processing of β-carboxyl-terminal fragment. *J. Biol. Chem.* **289,** 5109-5121.

60. Monné M., Hermansson M., and von Heijne G. (1999) A turn propensity of scale for transmembrane helices. *J Mol Bio.* **288,** 141-145.

61. Munter L.M., Voigt P., Harmeier A., Kaden D., Gottschalk K.E., Weise C., Pipkorn R., Schaefer M., Langosch D., and Multhaup G. (2007) GXXXG motifs within the amyloid precursor protein transmembrane sequence are critical for the etiology of Aβ42. *EMBO J*. **26**, 1702-1722.

62. Niimura M., Isoo N., Takasugi N., Tsuruoka M., Ui-Tei K., Saigo K., Morohashi Y., Tomita T., and Iwatsubo T. (2005) Aph-1 contributes to the stabilization and trafficking of the γ-secretase complex through mechanisms involving intermolecular and intramolecular interactions. *J. Biol. Chem.* **280,** 12967–12975.

63. Okochi M., Tagami S., Yanagida K., Takami M., Kodama T.S., Mori K., Nakayama T., Ihara Y., and Takeda M. (2013) γ-Secretase Modulators and Presenilin 1 Mutants Act Differently on Presenilin/γ-Secretase Function to Cleave Aβ42 and Aβ43. *Cell Rep.* **3,** 42-51.

64. Pettegrew J.W., Panchalingam K., Hamilton R.L., and McClure R.J. (2001) Brain membrane phospholipid alterations in Alzheimer's disease. *Neurochem Res.* **26,** 771–782.

65. Piao Y., Kimura A., Urano S., Saito Y., Taru H., Yamamoto T., Hata S., and Suzuki T. (2013) Mechanism of intramembrane cleavage of alcadeins by γ-secretase. *PLoS One.* **8,** e62431.

66. Pitsi D., Kienlen-Campard P., and Octave J.N. (2002) Failure of the interaction between presenilin 1 and the substrate of γ-secretase to produce Aβ in insect cells. *Journal of Neurochemistry*. **83,** 390–399.

67. Priller C., Bauer T., Mitteregger G., Krebs B., Kretzschmar H.A., and Herms J. (2006) Synapse formation and function is modulated by the amyloid precursor protein. *J. Neurosci.* **26**, 7212-7221.

68. Prince M., Albanese E., Guerchet M., and Prina M. (2014) Dementia and risk reduction: An analysis of protective and modifiable factors, Alzheimer's Disease International, London, http://www.alz.co.uk/research/WorldAlzheimerReport2014.pdf

69. Qi-Takahara Y., Morishima-Kawashima M., Tanimura Y., Dolios G., Hirotani N., Horikoshi Y., Kametani F., Maeda M., Saido T.C., Wang R., and Ihara Y. (2005) Longer Forms of Amyloid β Protein: Implications for the Mechanism of Intramembrane Cleavage by γ-Secretase. *J. Neurosci.* **25**, 436-445.

70. Russ W.P., and Engelman D.M. (2000) The GxxxG motif: a frame work for transmembrane helix-helix association. *J. Mol. Biol.* **296**, 911-919.

71. Saito T., Suemoto T., Brouwers N., Sleegers K., Funamoto S., Mihira N., Matsuba Y., Yamada K., Nilsson P., Takano J., Nishimura M., Iwata N., Van Broeckhoven C., Ihara Y., and Saido T.C. (2011) Potent amyloidogenicity and pathogenicity of Aβ43. *Nat Neurosci.* **14,** 1023-1032.

72. Schägger H. (2001) Blue-native gels to isolate protein complex from mitochondria. *Methods Cell Biol.* **65**, 231-244.

73. Schägger H., Cramer W.A., and von Jagow G. (1994) Analysis of molecular masses and oligomeric states of protein complexes by blue native electrophoresis and isolation of membrane protein complexes by two-dimensional native electrophoresis. *Anal. Biochem.* **217,** 220-230.

74. Schägger H., and von Jagow G. (1991) Blue native electrophoresis for isolation of membrane protein complexes in enzymatically active form. *Anal. Biochem.* **199**, 223-231.

75. Scheinfeld M.H., Ghersi E., Laky K., Fowlkes B.J., and D'Adamio L. (2002) Processing of β-Amyloid Precursor-like Protein-1 and -2 by γ-Secretase Regulates Transcription. *J. Biol. Chem.* **277,** 44194–44201.

76. Selkoe D.J. (1994) Cell biology of the amyloid β-protein precursor and the mechanism of Alzheimer's disease. *Annu Rev Cell Biol.* **10,** 373-403.

77. Selkoe D.J., and Kopan R. (2003) Notch and presenilin: regulated intramembrane proteolysis links development and degeneration. *Annu. Rev. Neurosci*. **6**, 565-597.

78. Selkoe D.J., Podlisny M.B., Joachim C.L., Vickers E.A., Lee G., Fritz L.C, and Oltersdorf T. (1988) Beta-amyloid precursor protein of Alzheimer disease occurs as 110- to 135-kilodalton membrane-associated proteins in neural and nonneural tissues. *Proc Natl Acad Sci.* **85,** 7341-7345.

79. Shah S., Lee S.F., Tabuchi K., Hao Y.H., Yu C., LaPlant Q., Ball H., Dann C.E. 3rd, Südhof T., and Yu G. (2005) Nicastrin functions as a γ-secretase-substrate receptor *Cell.* **122,** 435-447.

80. Shoji M., Golde T.E., Ghiso J., Cheung T.T., Estus S., Shaffer L.M., Cai X.D., McKay D.M., Tintner R., Frangione B., and Younkin S.G. (1992) Production of the Alzheimer amyloid beta protein by normal proteolytic processing. *Science.* **258,** 126-129.

81. Sinha S., Anderson J.P., Barbour R., Basi G.S., Caccavello R., Davis D., Doan M., Dovey H.F., Frigon N., Hong J., Jacobson-Croak K., Jewett N., Keim P., Knops J., Lieberburg I., Power M., Tan H., Tatsuno G., Tung J., Schenk D., Seubert P., Suomensaari S.M., Wang S., Walker D., Zhao J., McConlogue L., and John V. (1999) Purification and cloning of amyloid precursor protein β-secretase from human brain. *Nature*. **402,** 537-540.

82. Soba P., Eggert S., Wagner K., Zentgraf H., Siehl K., Kreger S., Lower A., Langer A., Merdes G., Paro R., Masters C.L., Muller U., Kins S., and Beyreuther K (2006) Homo- and hetero-dimerization of APP family members promotes intercellular adhesion. *EMBO J* **24,** 3624-3634.

83. Spasic D. and Annaert W. (2008) Building γ-secretase: the bits and pieces. *J. Cell Sci.* **121**, 413-420.

84. Steiner H., Fluhrer R., and Haass C. (2008) Intramembrane proteolysis by γ-secretase. *J. Biol. Chem.* **283**, 29627-29631.

85. Steiner H., Winkler E., and Haass C. (2008) Chemical cross-linking provides a model of the γ-secretase complex subunit architecture and evidence for close proximity of the C-terminal fragment of presenilin with APH-1. *J. Biol. Chem.* **279**, 41340-41345.

86. Stelzmann R.A., Schnitzlein H.N., and Murtagh F.R. (1995) An English translation of Alzheimer's 1907 paper,"uber eine eigenartige erkankung der hirnrinde. *Clin. Anat.* **8,** 429−431.

87. Swerdlow P. S., Finley D., and Varshavsky A. (1986) Enhancement of immunoblot sensitivity by heating of hydrated filters. *Anal. Biochem.* **156,** 147–153.

88. Takagi-Niidome S., Sasaki T., Osawa S., Sato T., Morishima K., Cai T., Iwatsubo T., and Tomita T. (2015) Cooperative roles of hydrophilic loop 1 and the C-terminus of presenilin 1 in the substrate-gating mechanism of γ-secretase. *Neurosci.* **35,** 2646-2656.

89. Takami M. and Funamoto S. (2012) γ-Secretase-Dependent Proteolysis of Transmembrane Domain of Amyloid Precursor Protein: Successive Tri- and Tetrapeptide Release in Amyloid β-Protein Production. *Int. J. Alzheimers Dis*. doi: 10.1155/2012/591392.

90. Takami M., Nagashima Y., Sano Y., Ishihara S., Morishima-Kawashima M., Funamoto S., and Ihara Y. (2009) γ-Secretase: Successive Tripeptide and Tetrapeptide Release from the Transmembrane Domain of β-Carboxyl Terminal Fragment. *J. Neurosci.* **29,** 13042-13052.

91. Takasugi N., Tomita T., Hayashi I., Tsuruoka M., Niimura M., Takahashi Y., Thinakaran G., and Iwatsubo T. (2003) The role of presenilin cofactors in the γ-secretase complex. *Nature.* **422,** 438–441.

92. Thinakaran G., Borchelt D.R., Lee M.K., Slunt H.H., Spitzer L., Kim G., Ratovitsky T., Davenport F., Nordstedt C., Seeger M., Hardy J., Levey A.I., Gandy S.E., Jenkins N.A., Copeland N.G., Price D.L., and Sisodia S.S. (1996) Endoproteolysis of Presenilin1 and Accumulation of Processed Derivatives In Vivo. *Neuron.* **17,** 181-190.

93. Thinakaran G., and Koo. E.H. (2008) Amyloid precursor protein trafficking, processing, and function. *J. Biol. Chem.* **283**, 29615-29619.

94. Tomita T. (2014) Molecular mechanism of intramembrane proteolysis by γ-secretase. *J. Biol. Chem.* **156,** 195-201.

95. Troyanovsky R.B., Sokolov E., and Troyanovsky S.M. (2003) Adhensive and lateral E-cadherin dimers are mediated by the same interface. *Mol Cell Biol* **23,** 7965–7972.

96. Vassar R., Bennett B.D., Babu-Khan S., Kahn S., Mendiaz E.A., Denis P., Teplow D.B., Ross S., Amarante P., Loeloff R., Luo Y., Fisher S., Fuller J., Edenson S., Lile J., Jarosinski M.A., Biere A.L., Curran E., Burgess T., Louis J.C., Collins F., Treanor J., Rogers G., and Citron M. (1999) β-Secretase Cleavage of Alzheimer's Amyloid Precursor Protein by the Transmembrane Aspartic Protease BACE. *Science.* **286**, 735–741.

97. Watson H. (2015) Biological membranes. *Essays Biochem.* **59,** 43-69.

98. Wittig I., Braun H.P., and Schägger H. (2006) Blue native PAGE. *Nat. Protoc.* **1**, 418-428.

99. Wolozin B. (2004) Cholesterol and the biology of Alzheimer’s disease. *Neuron.* **41,** 7-10.

100. Wu J., Anwyl R., and Rowan M.J. (1995) β-amyloid-(1-40) increases long-term potentiation in rat hippocampus in vitro. *Eur J Pharmacol.* **284,** R1-R3.

101. Yagishita S., Morishima-Kawashima M., Ishiura S., and Ihara Y. (2008) Aβ46 is Processed to Aβ40 and Aβ43, but Not to Aβ42, in the Low Density Membrane Domains. *J. Biol. Chem.* **283,** 733-738.

102. Yan R., Bienkowski M.J., Shuck M.E., Miao H., Tory M.C., Pauley A.M., Brashier J.R., Stratman N.C., Mathews W.R., Buhl A.E., Carter D.B., Tomasselli A.G., Parodi L.A., Heinrikson R.L., and Gurney M.E. (1999) Membrane-anchored aspartyl protease with Alzheimer's disease β-secretase activity. *Nature.* **402,** 533-537.

103. Yan Y., Xu T.H., Harikumar K.G., Miller L.J., Melcher K., and Xu H.E. (2017) Dimerization of the transmembrane domain of amyloid precursor protein is determined by residues around the γ-secretase cleavage sites. *J. Biol. Chem.* **292,** 15826–15837.

104. Younkin S.G. (1995) Evidence that Aβ42 is the real culprit in alzheimer's disease. *Ann Neurol.* **37,** 287-288.

105. Young-Pearse T.L., Bai J., Chang R., Zheng J.B., LoTurco J.J., and Selkoe D.J. (2007) A critical function for β-amyloid precursor protein in neuronal migration revealed by in utero RNA interference. *J. Neurosci.* **27,** 14459-14469.

106. Yu G., Nishimura M., Arawaka S., Levitan D., Zhang L., Tandon A., Song Y.Q., Rogaeva E., Chen F., Kawarai T., Supala A., Levesque L., Yu H., Yang D.S., Holmes E., Milman P., Liang Y., Zhang D.M., Xu D.H., Sato C., Rogaev E., Smith M., Janus C., Zhang Y., Aebersold R., Farrer L.S., Sorbi S., Bruni A., Fraser P., and St George-Hyslop P. (2000). Nicastrin modulates presenilin-mediated notch/glp-1 signal transduction and βAPP processing. *Nature*. **407,** 48–54.

107. Zhao G., Mao G., Tan J., Dong Y., Cui M.Z., Kim S.H., and Xu X. (2004) Identification of a New Presenilin-dependent ζ-cleavage Site within the Transmembrane Domain of Amyloid Precursor Protein. *J. Biol. Chem.* **279,** 50647–50650.